



OPEN

Cyclosporine-induced kidney damage was halted by sitagliptin and hesperidin via increasing Nrf2 and suppressing TNF- α , NF- κ B, and Bax

Ahmed M. Abd-Eldayem^{1,2}✉, Sohayla Mahmoud Makram², Basim Anwar Shehata Messiha³, Hanan H. Abd-Elhafeez⁴ & Mustafa Ahmed Abdel-Reheim^{3,5}

Cyclosporine A (CsA) is employed for organ transplantation and autoimmune disorders. Nephrotoxicity is a serious side effect that hampers the therapeutic use of CsA. Hesperidin and sitagliptin were investigated for their antioxidant, anti-inflammatory, and tissue-protective properties. We aimed to investigate and compare the possible nephroprotective effects of hesperidin and sitagliptin. Male Wistar rats were utilized for induction of CsA nephrotoxicity (20 mg/kg/day, intraperitoneally for 7 days). Animals were treated with sitagliptin (10 mg/kg/day, orally for 14 days) or hesperidin (200 mg/kg/day, orally for 14 days). Blood urea, serum creatinine, albumin, cystatin-C (CYS-C), myeloperoxidase (MPO), and glucose were measured. The renal malondialdehyde (MDA), glutathione (GSH), catalase, and SOD were estimated. Renal TNF- α protein expression was evaluated. Histopathological examination and immunostaining study of Bax, Nrf-2, and NF- κ B were performed. Sitagliptin or hesperidin attenuated CsA-mediated elevations of blood urea, serum creatinine, CYS-C, glucose, renal MDA, and MPO, and preserved the serum albumin, renal catalase, SOD, and GSH. They reduced the expressions of TNF- α , Bax, NF- κ B, and pathological kidney damage. Nrf2 expression in the kidney was raised. Hesperidin or sitagliptin could protect the kidney against CsA through the mitigation of oxidative stress, apoptosis, and inflammation. Sitagliptin proved to be more beneficial than hesperidin.

Keywords Cyclosporine, Sitagliptin, Hesperidin, Nephrotoxicity, Nrf2, NF- κ B

Cyclosporine A (CsA), an immunosuppressive drug, prevents allograft rejection in solid organ transplantation. CsA has also been used to treat autoimmune disorders including psoriasis and rheumatoid arthritis^{1–3}. However, a dangerous side effect that restricts its clinical usage is CsA nephrotoxicity⁴. Inflammatory cell infiltration, tubular shrinkage, arteriopathy, increased immunogenicity, and tubular interstitial fibrosis are the characteristics of the described CsA-evoked nephrotoxicity⁵. Although many different factors are involved in the pathophysiology of CsA-induced nephrotoxicity, oxidative stress is crucial to the onset and advancement of this disease. The basic signs of CsA renal injury are reactive oxygen species (ROS) overruns and associated lipid peroxidation or oxidative aberrations⁶. In this regard, CsA-treated human renal mesangial cells showed an overshooting of ROS^{7,8}.

Some data suggest that oxidative stress plays an important role in underlying nephrotoxicity, in particular, the superoxide (O_2^-) that is the most powerful free radical generated by nicotinamide adenine dinucleotide phosphate (NADPH) oxidase-1 (NOX1) present mainly in the kidney^{9,10}. Moreover, it has been observed that hypertensive patients receiving CsA medication have higher plasma hydroperoxide levels^{2,10}. Additionally, LLC-PK1 tubular cells have been identified as having decreased renal antioxidants like reduced glutathione^{2,11}.

¹Department of Medical Pharmacology, Faculty of Medicine, Assiut University, Assiut, Egypt. ²Department of Pharmacology, Faculty of Medicine, Merit University, Sohâg, Egypt. ³Department of Pharmacology and Toxicology, Faculty of Pharmacy, Beni-Suef University, Beni Suef, Egypt. ⁴Department of Cell and Tissue, Faculty of Veterinary Medicine, Assiut University, Assiut, Egypt. ⁵Department of Pharmaceutical Sciences, College of Pharmacy, Shaqra University, Shaqra, Saudi Arabia. ✉email: dr.ahmed2016@aun.edu.eg

The mechanisms of CsA-induced nephrotoxicity are multifactorial, with inflammatory events dominating the pathogenesis of this disorder^{12,13}. Conventionally, inflammation is considered an adaptive mechanism to remove invading cells and repair damaged tissue. However, an exaggerated inflammatory response and associated production of proinflammatory cytokines, including interleukin 1 beta (IL-1 β) and tumor necrosis factor-alpha (TNF- α), have been reported during the progression of kidney injury. TNF-alpha mRNA, dendritic cell count, and MHC class II antigen expression were all increased after receiving CsA treatment^{13,14}.

Also, cyclosporine could induce renal tissue damage by increasing the expression of inflammatory mediators such as TNF- α and tumor growth factor (TGF)- β . The produced TNF- α stimulates dendritic cell maturation, activates the innate immune responses, and enhances the production of diverse chemokines and cytokines, as occurs in lupus nephritis^{15,16}. TNF- α is a crucial immunoregulatory and proinflammatory cytokine with pleiotropic features, including the ability to trigger an inflammatory chain reaction that results in tissue damage. One of the transcription factors whose activation has been proposed to be associated with the expression of antioxidant enzymes is nuclear factor erythroid 2-related factor-2 (Nrf-2). Moreover, Nrf2 has been reported to be one of the main regulators of the glutathione S-transferase family, which induces detoxification by increasing the cytosolic concentration of GSH. Furthermore, many studies indicated that the expression of Nrf-2 prevented excessive inflammatory responses in the renal tissue exposed to cyclosporine¹⁷⁻¹⁹. The nuclear factor-kappa B pathway has long been considered a prototypical proinflammatory signaling pathway, largely based on the role of NF- κ B in the expression of proinflammatory genes including cytokines, chemokines, and adhesion molecules²⁰. Also, elevated renal expressions of inducible nitric oxide synthase (iNOS) and nuclear factor kappa B (NF- κ B) were noticed due to CsA administration²¹.

DPP-4 inhibitors have been shown to reduce proteinuria by reducing renal inflammatory indicators in diabetics. Numerous investigations were carried out to demonstrate the feasibility of the same effects in non-diabetic nephropathies. These investigations supported the ability of DPP-4 inhibitors to decrease proteinuria without having an impact on glucose metabolism by showing an improvement in several renal inflammatory markers^{22,23}. Sitagliptin, a dipeptidyl peptidase 4 inhibitor, was the first in its class to receive approval from the US FDA in 2006 for the treatment of type 2 diabetes mellitus. In clinical trials, sitagliptin was usually well tolerated, had a negligible risk of hypoglycemia, had no discernible impact on body weight, and could be used in chronic kidney disease^{24,25}. Sitagliptin might have a major role in preventing diabetic nephropathy (DN) evolution due to its anti-inflammatory and antiapoptotic properties^{26,27}.

Additionally, sitagliptin improved renal functions and histopathological changes, impeded inflammation, oxidative stress, tubulointerstitial transdifferentiation, and fibrosis, and upregulated the PI3K/AKT pathway, which highlights its renoprotective effects in many rat models of diabetic nephropathy²⁸⁻³⁰. Sitagliptin has been shown to have nephroprotective, antioxidant, and anti-inflammatory impacts. Consequently, sitagliptin administration can limit the nephrotoxic effects of deltamethrin through its free radical-scavenging and strong antioxidant activity³¹. In addition, sitagliptin exhibited potent nephroprotective properties against the nephrotoxicity induced by methotrexate³², gentamicin³³, acute IR injury^{34,35}, and adenine-induced kidney disease in rats³⁶.

Hesperidin, a bioflavonoid, is present in large amounts in citrus fruits. Its use has been linked to several health benefits, including antioxidant, antibacterial, antimicrobial, anti-inflammatory, and anticarcinogenic properties³⁷. Hesperidin protected the renal and lung tissues of rats after ischemia-reperfusion injury³⁸. Hesperidin afforded protection against sodium fluoride-induced liver, kidney, and cardiac damage in rats through antioxidant, anti-inflammatory, anti-apoptotic, and anti-autophagic mechanisms^{39,40}. Similarly, hesperidin administration protected the liver and kidneys against the destructive effects of sodium arsenite⁴¹ and acrylamide⁴². In rats subjected to paclitaxel-induced hepatorenal toxicity, hesperidin significantly decreased mRNA expression levels of NF- κ B, TNF-, IL-1, IL-6, Caspase-3, and Bax, while increasing levels of Nrf2, HO-1, and Bcl-2 in the kidney and liver⁴³.

Numerous investigations using kidney injury models, such as AlCl₃-induced renal damage⁴⁴, cisplatin-induced nephrotoxicity⁴⁵, and 5-fluorouracil-induced renal dysfunction⁴⁶, showed the plausible renoprotective action of hesperidin. Additionally, hesperidin has been identified as a novel and promising therapeutic agent capable of modifying several cardiovascular disease risk factors (CVDs). Furthermore, in diabetic mice, hesperidin showed lower blood sugar and reduced inflammation⁴⁷.

This study aimed to investigate the potential protective effects of sitagliptin and hesperidin against the nephrotoxicity caused by CsA and to elucidate the possible mechanisms involved. Evaluation of the nephrotoxicity and impact of the chosen therapies was done through biochemical, pathological, and protein expression investigations. Additionally, we want to compare the protective effects of sitagliptin to hesperidin as a nephroprotective tool in CsA-induced kidney injury.

Results

The serum levels of urea and creatinine

As shown in Fig. 1, CsA administration significantly elevated the serum levels of urea (Fig. 1A) and creatinine (Fig. 1B) as compared to normal control values ($p < 0.0001$). Using sitagliptin with CsA greatly reduced the rise in serum levels of urea and creatinine ($p < 0.0001$) as compared to CsA-treated rats. Hesperidin coadministration with CsA considerably reduced the increase in blood levels of urea and creatinine ($p < 0.0001$). Sitagliptin and hesperidin administered individually produced no significant changes in these biochemical parameters versus control rats given the vehicle. A comparative look at the figure indicates that sitagliptin treatment was greater than hesperidin in the correction of serum parameters, indicating its preservative effect on renal tissue.

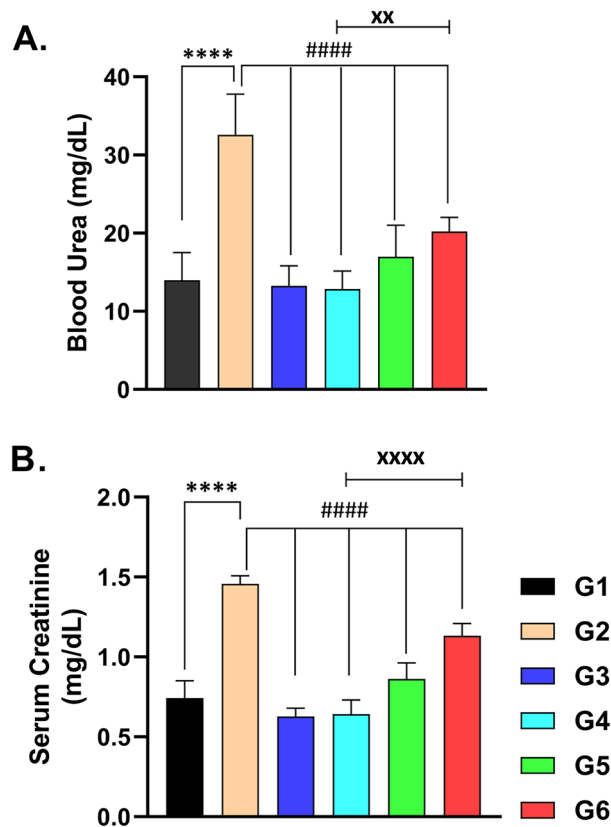


Figure 1. Effects of administration of cyclosporine, sitagliptin, and hesperidin on Blood urea (A) and serum creatinine (B) levels: data represented as mean \pm SEM (n = 6). (G1 = Control, G2 = CsA-treated rats, G3 = Sitagliptin, G4 = Sitagliptin + CsA, G5 = Hesperidin, G6 = Hesperidin + CsA). **** ($p < 0.0001$) versus G1 rats, #### ($p < 0.0001$) versus G2 rats, xx ($p < 0.01$) & xxx ($p < 0.0001$) versus G6 rats.

The levels of serum Albumin (ALB), blood glucose, serum myeloperoxidase (MPO), and serum cystatin-C (CYS-C)

For serum albumin, cyclosporine A administration to rats substantially decreased its levels in comparison to control rats (Fig. 2A, $p < 0.0001$). The coadministration of sitagliptin with CsA gave rise to a significant preservation of albumin levels compared to those of CsA-treated rats (Fig. 2A, $p < 0.0001$) and to those that received a combination of CsA and hesperidin. As illustrated in Fig. 2, CsA treatment showed a deleterious impact on the levels of glucose, myeloperoxidase (MPO), and cystatin-C (CYS-C), as they were elevated significantly (Fig. 2B–D, respectively, $p < 0.0001$). Treatment with sitagliptin or hesperidin attenuated the elevation of the aforementioned parameters considerably in reference to CsA-treated animals ($p < 0.0001$). Furthermore, treatment with sitagliptin or hesperidin individually showed no significant changes in the levels of the biomarkers compared to the control rats. Such results explain the reno-protective activities of sitagliptin or hesperidin against CsA-induced damage to kidney cells. For the above-mentioned serum markers, sitagliptin administration with CsA produced a significant effect compared to hesperidin administration with CsA (Fig. 2).

Kidney MDA and GSH

The renal tissue of rats that received CsA showed a significant elevation of the biochemical marker of lipid peroxidation (MDA) compared to normal control rats ($p < 0.0001$) (Fig. 3A,B). Coadministration of sitagliptin with CsA resulted in a significant attenuation of CsA-induced MDA rise ($p < 0.0001$) as compared to CsA-treated rats. The renal tissue glutathione (GSH) has been reduced upon CsA treatment, indicating its depletion in comparison to control animals ($p < 0.0001$). As noted in Fig. 3B, the use of sitagliptin or hesperidin with CsA produced the preservation of kidney GSH, maintaining an antioxidant defense mechanism ($p < 0.0001$). The use of sitagliptin or hesperidin alone had no significant impact on the MDA and GSH levels, which were near normal with these medications. It is noteworthy to mention that sitagliptin has a greater effect compared to the use of hesperidin against CsA-induced oxidative insult in the kidney (Fig. 3A,B, $p < 0.05$).

Kidney CAT activity

Measuring the CAT activity revealed the considerable defect produced using CsA in the kidney tissues, comparing this to normal kidneys in rats that received the vehicle (Fig. 3C, $p < 0.0001$). Interestingly, administering sitagliptin or hesperidin concomitantly with CsA preserved renal CAT activity (Fig. 3C, $p < 0.0001$). The use of

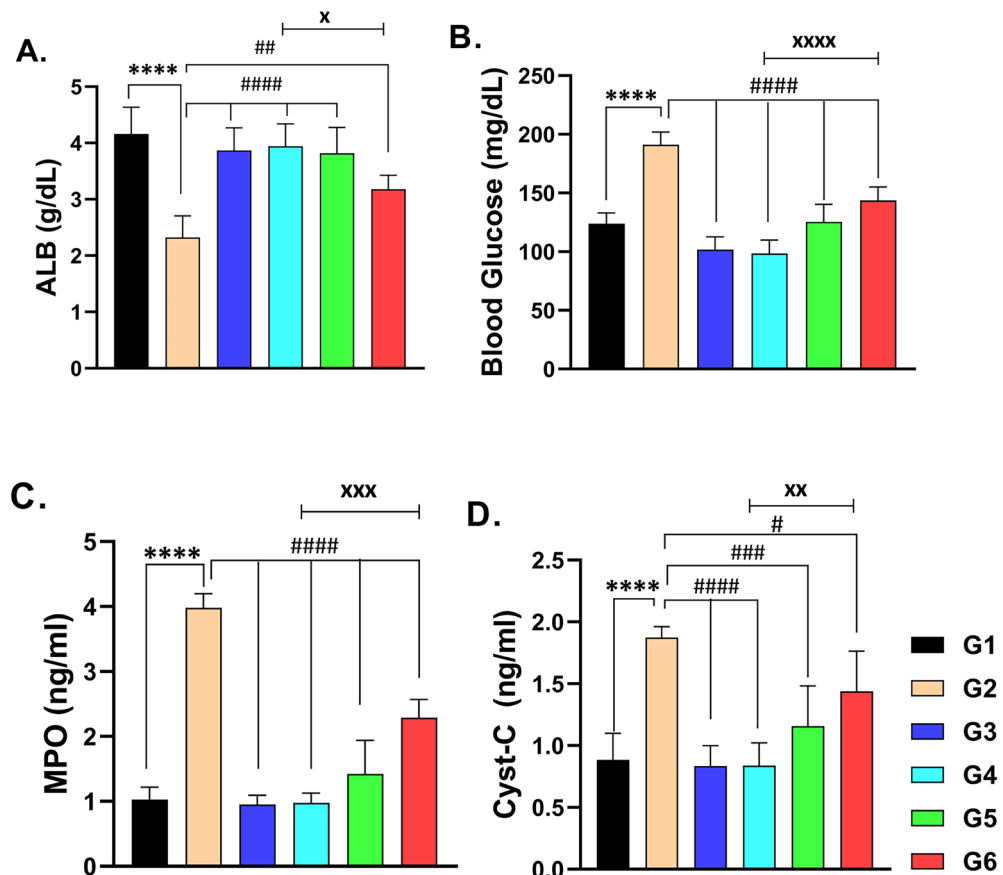


Figure 2. The effects of administration of cyclosporine, sitagliptin, and hesperidin on the serum levels of albumin (ALB) (A), blood glucose (B), myeloperoxidase (MPO) (C) and cystatin-C (Cyst-C) (D). data represented as mean \pm SEM (n = 6). (G1 = Control, G2 = CsA-treated rats, G3 = Sitagliptin, G4 = Sitagliptin + CsA, G5 = Hesperidin, G6 = Hesperidin + CsA). **** ($p < 0.0001$) versus G1 rats, # ($p < 0.05$), ## ($p < 0.01$), ### ($p < 0.001$) & #### ($p < 0.0001$) versus G2 rats, xx ($p < 0.01$) & xxx ($p < 0.0001$) versus G6 rats.

sitagliptin or hesperidin alone produced no significant effect on the CAT activity in the renal tissue. Comparing sitagliptin with CsA to hesperidin with CsA brought out the ability of sitagliptin to have a higher beneficial effect ($p < 0.05$).

Kidney SOD activity

When compared to control rats, CsA-treated animals showed a lowered SOD activity in the renal tissue (Fig. 3D, $p < 0.0001$). SOD activity was preserved near normal by using sitagliptin or hesperidin with CsA when compared to rats with CsA-induced nephrotoxicity ($p < 0.0001$). As noticed in Fig. 3D, the use of sitagliptin or hesperidin resulted in insignificant changes in SOD activity compared to normal rats. Additionally, sitagliptin preserved SOD activity more than hesperidin did when given with CsA.

Renal tissue TNF- α

To further substantiate the protective effects associated with sitagliptin or hesperidin against CSA-induced nephrotoxicity in rats, protein expression of TNF- α was assessed. Notably, CsA significantly induced the expression of TNF- α by approximately 200% relative to the control values. The expression of TNF- α in the kidney tissue was higher in rats receiving CsA compared to control animals. The administration of sitagliptin or hesperidin with CsA resulted in a significant reduction in TNF- α expression in the kidney tissues when compared to CsA-treated rats. When administered alone, sitagliptin or hesperidin produced no significant changes compared to control rats. It is to be mentioned that sitagliptin treatment was slightly superior to hesperidin administration when given with CsA (Fig. 4).

Histopathological examination

The photomicrographs of kidney sections from the control group of rats exhibited normal glomeruli with an intact Bowman's capsule, as well as normal proximal convoluted tubules and distal convoluted tubules in the renal cortex (Fig. 5). The renal cortex sections of rats that received CsA exhibited observable manifestations such as glomerular shrinkage, a decrease in Bowman's space, and renal corpuscles. The lining epithelium of several tubules exhibited disruption, resulting in dilation and large necrotic regions. The renal tubules displayed dilation,

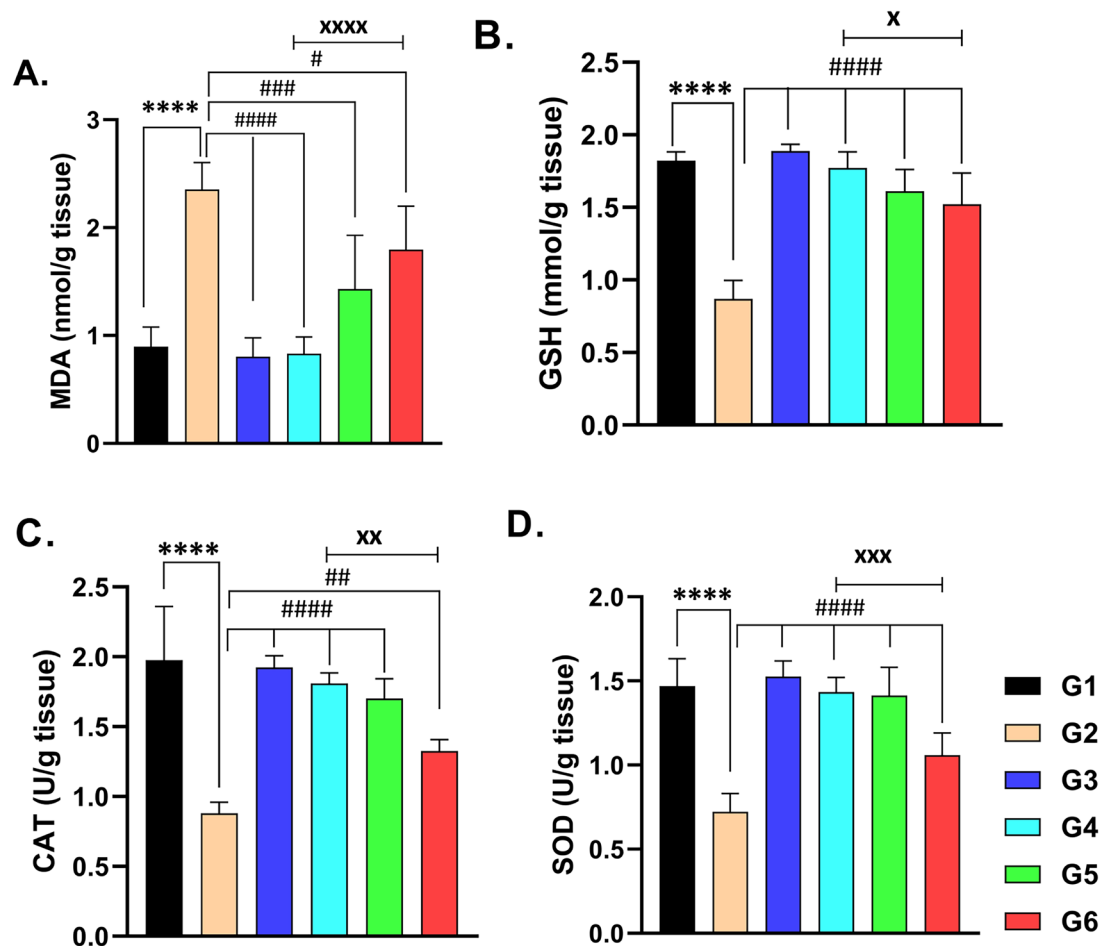


Figure 3. The renal tissue levels of MDA (A) and GSH (B) and renal tissue activities of CAT (C) and SOD (D) on administration of CsA, Sitagliptin, and hesperidin. Data represented as mean \pm SEM ($n=6$). MDA = Malondialdehyde, GSH = reduced glutathione, CAT = Catalase, SOD = Superoxide dismutase & CsA = Cyclosporine A. (G1 = Control, G2 = CsA-treated rats, G3 = Sitagliptin + CsA, G4 = Sitagliptin + CsA, G5 = Hesperidin, G6 = Hesperidin + CsA). **** ($p < 0.0001$) significant difference from normal control rats, # ($p < 0.05$), ## ($p < 0.01$), ### ($p < 0.001$) & #### ($p < 0.0001$) significant difference from CsA-treated rats and ^x ($p < 0.05$), ^{xx} ($p < 0.01$), ^{xxx} ($p < 0.001$) & ^{xxxx} ($p < 0.0001$) significant difference from (Hesperidin + CsA)-treated rats.

accompanied by the presence of interstitial inflammatory cells surrounding blood vessels, vascular congestions, and interstitial hemorrhage and the detection of macrophage giant cells (Fig. 6). These findings were greatly obvious when compared to control animals (Fig. 6 vs. Fig. 5). Examination of the kidney sections from other groups revealed that sitagliptin or hesperidin administration was not associated with significant pathological findings as compared to CsA-treated rats. When sitagliptin or hesperidin were given with CsA, they attenuated the development of pathological kidney damage compared to the nephrotoxicity group, and this was more obvious regarding sitagliptin treatment with CsA (Fig. 7).

The histological measurements uncovered the shrinkage of the renal corpuscles in the rats that received CsA when compared to control rats. The glomerular diameter and capsular space were markedly lower in the nephrotoxicity group than in healthy rats. Treatment with sitagliptin, hesperidin alone, or coadministered to CsA resulted in near-to-normal glomerular diameter and capsular space diameter (Figs. 8 and 9).

The present study involved the determination of the collagenous fibers using histomorphometric analysis as well as the quantification of fibrosis percentage in kidney sections. This analysis is conducted using the Sirius Red stain (Fig. 10) and the Periodic Acid-Schiff (PAS) stain (Fig. 11) to assess the percentage reaction in the kidney sections. The data analysis is represented as means \pm standard error (SE) and is visually depicted in Figs. 8M and 9M. The fibrosis and PAS stain intensity were increased in the CsA group, followed by a significant decrease in various treatment groups, and nearly returned to the control level. Furthermore, it was noticed that sitagliptin administration with CsA showed improved histological outcomes when compared to hesperidin treatment.

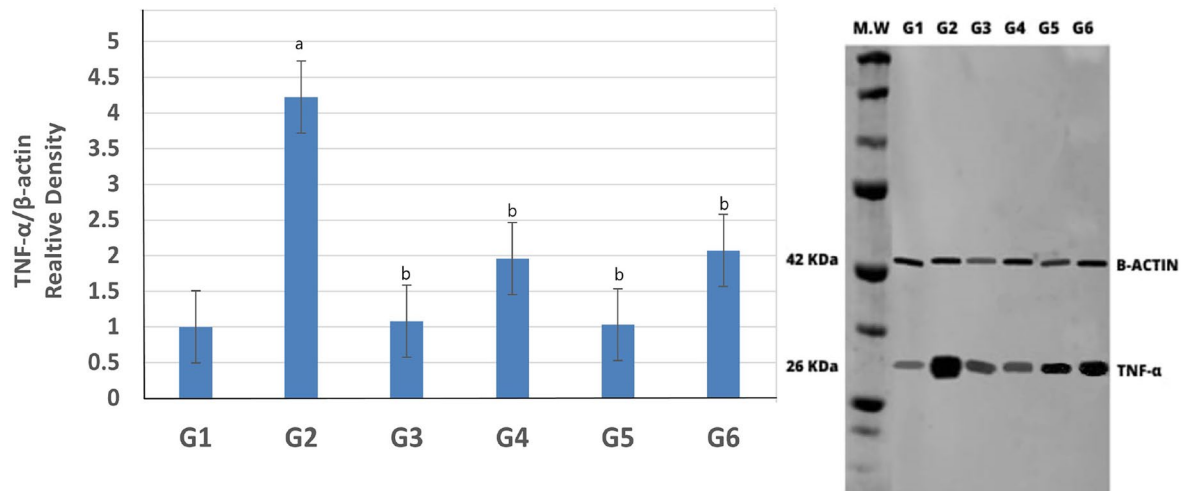


Figure 4. Effect of sitagliptin and hesperidin on expression of TNF- α in CsA treated rats. Immunoblotting for the target molecule of TNF- α showing the effects of sitagliptin and hesperidin in CsA-treated rats. Bar graphs show the expression levels of TNF- α . B-actin was used as the internal control. (G1 = Control, G2 = CsA-treated rats, G3 = Sitagliptin, G4 = Sitagliptin + CsA, G5 = Hesperidin, G6 = Hesperidin + CsA). ^a($p < 0.001$) compared to the control group, and ^b($p < 0.05$) compared to the CsA group.

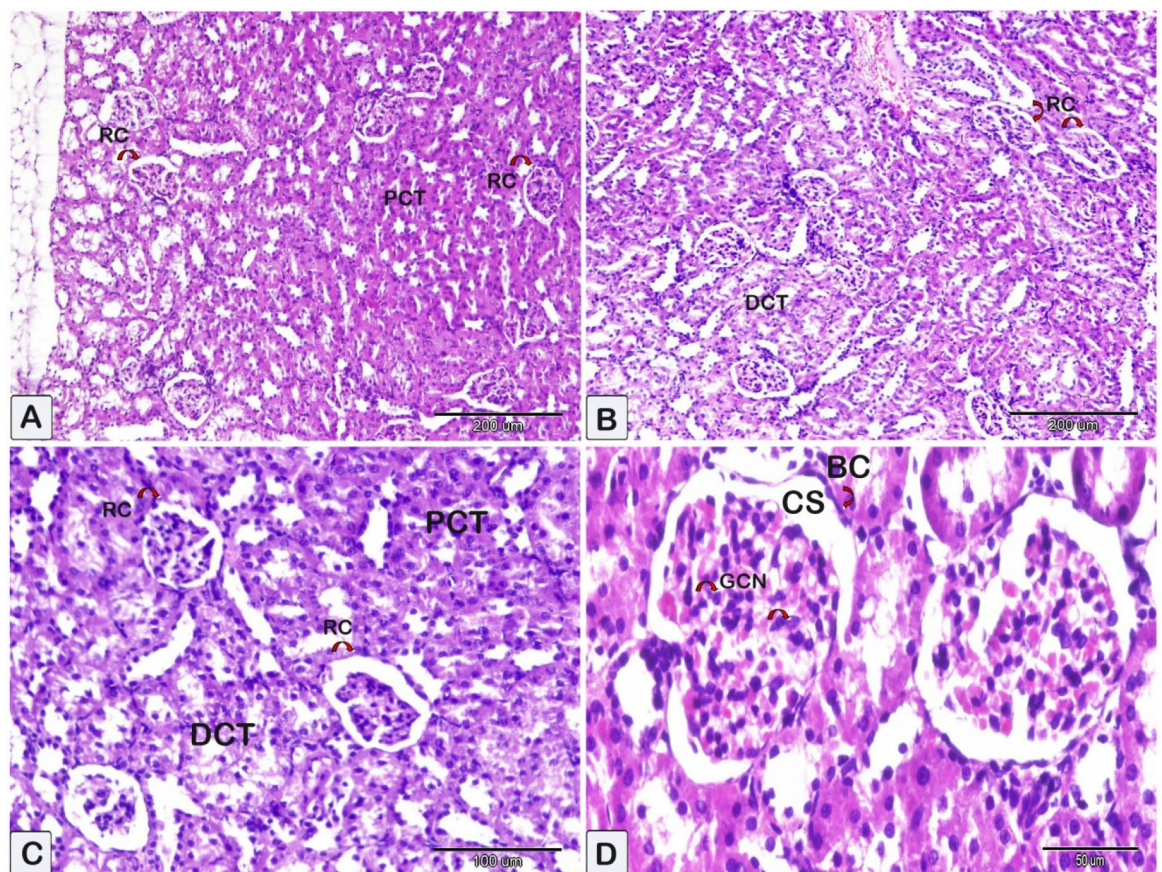


Figure 5. Representative photomicrographs of paraffin sections of kidney tissue obtained from the control group. These sections were stained with hematoxylin and eosin (HE). Microscopic examinations of the kidney tissues from control rats that received the vehicle revealed that the renal glomeruli and proximal and distal convoluted tubules had normal histological appearances. (A–D): The renal corpuscle (RC), consisting of Bowman's capsules (BC), demonstrates well-defined and consistent structural features. A typical epithelial cell with proximal (PCT) and distal convoluted tubules (DCT) is observed. The abundance of glomerular cell nuclei (GCN, shown by curved arrows) is notable. (CS) referred to capsular space.

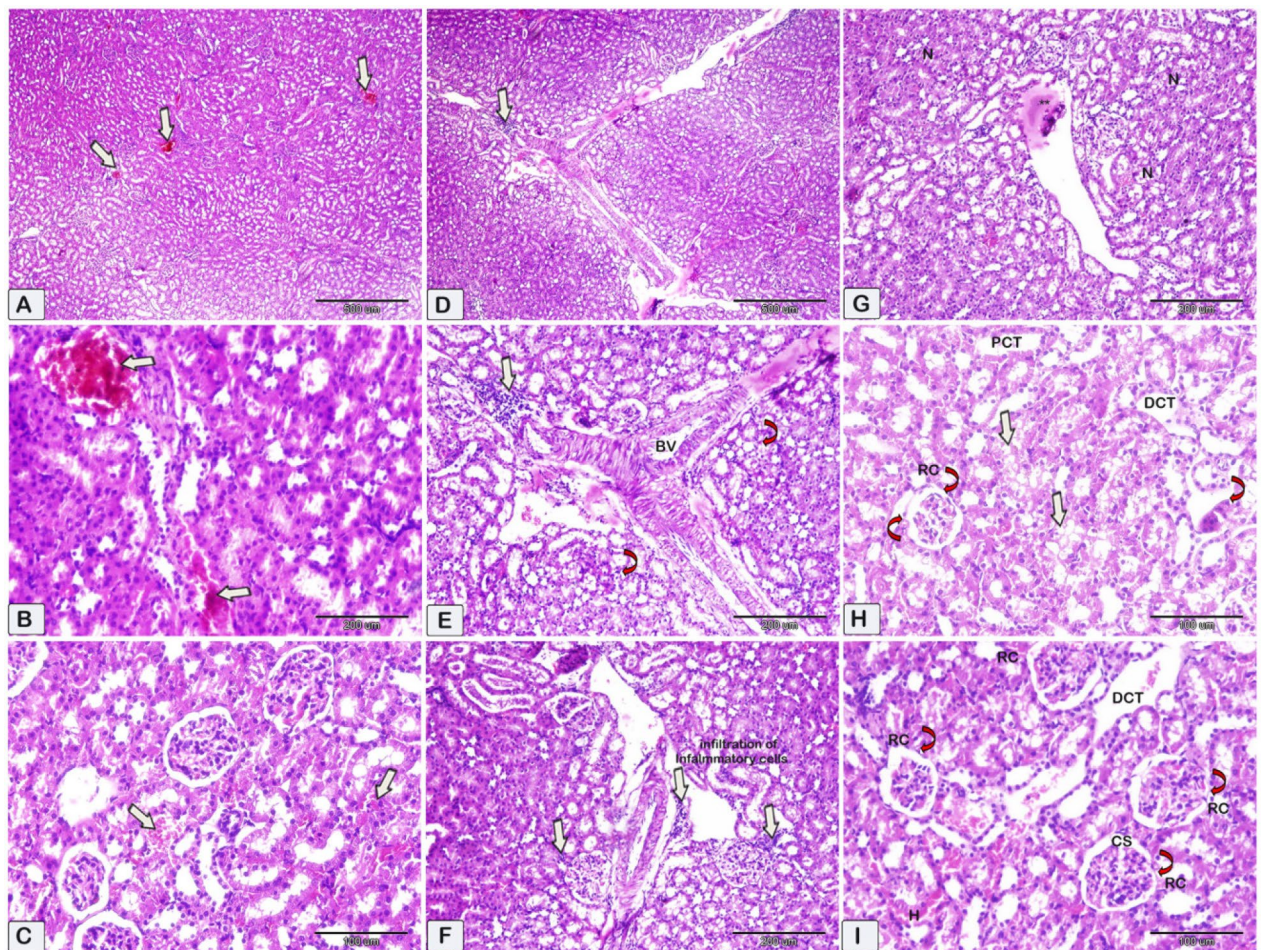


Figure 6. Representative photomicrographs of paraffin sections of kidney tissue obtained from the nephrotoxicity group (CsA group). These sections were stained with hematoxylin and eosin (HE) to visualize the tissue. (A,B) Vascular congestion and (C) Interstitial hemorrhages (shown by white arrows). The observed pathological findings include perivascular inflammatory cell infiltration, shown by the presence of white arrows surrounding blood vessels, as well as tubular degeneration accompanied by necrosis of epithelial cells, as denoted by the curved arrows. (D–I) the presence of necrosis in kidney tissue (N) is observed, namely in the proximal (PCT) and distal convoluted tubules (DCT). This necrosis is accompanied by a reduction in the size of the glomeruli within the renal corpuscle (RC, indicated by curved arrows) and a narrowing of the capsular space (CS). Additionally, there is evidence of interstitial hemorrhage (H) in the shown image in Figure (I). Macrophage Ginat cells were observed in Figure H (red curved arrow).

Immunohistochemical examination

Renal Nrf2

Immunostaining of renal tissue demonstrated observable levels of Nrf2 expression in the control rats (Fig. 12A). Sections of the CsA group (Fig. 12B) show renal tubular cells' cytoplasm and nuclei exhibit faint immunoreaction of Nrf2. Treatment with sitagliptin or hesperidin revealed near-to-control stained immune-reactive cells of renal tissues (Fig. 12C,E). Co-administration of sitagliptin to CsA showed enhanced Nrf2 expression as compared to CsA-treated rats (Fig. 12D). Furthermore, the presence of hesperidin along with CsA gave rise to obviously increased protein expression of Nrf2 (Fig. 12F). Additionally, it was detected that sitagliptin treatment with CsA produced a superior improvement in the protein expression of Nrf2 compared to hesperidin treatment with CsA.

Renal Bax

The expression of renal Bax was evaluated in the kidneys of the different groups. Glomerular and tubular cells from the nephrotoxicity group displayed an impressive positive cytoplasmic Bax reaction (Fig. 13B) compared to the negative reaction observed in the control group (Fig. 13A). Kidney sections of rats received sitagliptin or hesperidin uncovered renal tissues showed few immune-reactive cells with low Bax expression (Fig. 13C,E). The sitagliptin/CsA group's kidney sections had extremely low Bax immunoreactivity (Fig. 13D). The kidney tissues of the hesperidin/CsA group also showed decreased Bax expression and decreased brown staining intensity (Fig. 13F).

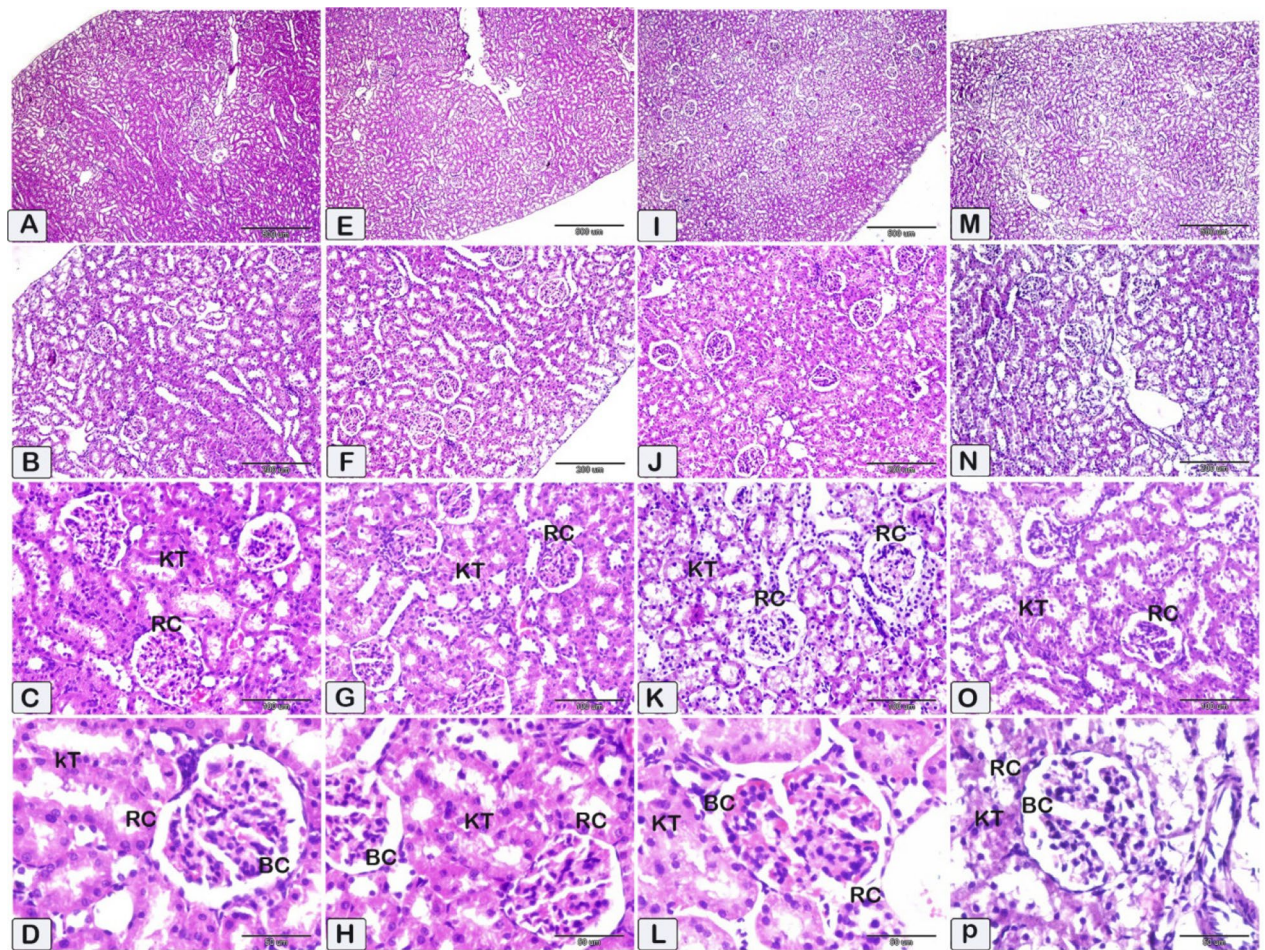


Figure 7. Displayed photomicrographs of paraffin sections of kidney tissue obtained from the treated groups and stained using hematoxylin and eosin (HE). (A–D) Figures at low and high magnifications of the kidney cortex of experimental group 3. (E–H) Figures at low and high magnifications of kidney cortex of experimental group 4. (I–L) Figures at low and high magnifications of the kidney cortex of experimental group 5. (M–P) Figures at low and high magnifications of the kidney cortex of experimental group 6 illustrate the typical histological features of kidney tubules and renal corpuscles within the cortex.

Renal NF- κ B

In the control group, a decrease in the levels of the NF- κ B protein is detected (Fig. 14A). The levels of NF- κ B protein expression were found to be significantly elevated in the CsA group compared to the control group (Fig. 14B). Subsequently, the expression levels of the treated group exhibited a reduction in the protein expressions of NF- κ B, as indicated by a low level of staining intensity and reaction in sections from rats received sitagliptin or hesperidin individually or with CsA (Fig. 14C–F). It was noticed that the immune reaction for NF- κ B was lower in the kidney sections of rats that received sitagliptin with CsA than in the kidney sections of rats that received hesperidin with CsA.

Discussion

The most serious limiting side effect of cyclosporine A (CsA) is nephrotoxicity⁴⁸, which can be manifested as either acute reversible kidney injury or chronic fibrotic renal dysfunction⁴⁹. It involves lesions such as tubular atrophy and interstitial fibrosis⁵⁰. Several interventions have been introduced to halt the pathogenesis of this dangerous complication during therapy with cyclosporine in patients with autoimmune diseases and organ transplantation³. Cyclosporine induces oxidative stress, which acts in various ways to cause tissue injury. Inflammatory cell infiltration into the kidney is a common finding, and this is initially associated with augmented expression and release of inflammatory cytokines and chemokines in the kidney⁵¹. In this work, we sought to determine if sitagliptin and hesperidin may shield rat kidneys from the damaging effects of cyclosporine. This was an attempt to protect kidney structure and function when using cyclosporine to treat an autoimmune illness or during organ transplantation. Urine and creatinine levels in the serum were significantly elevated in rats given cyclosporine. This was in line with numerous studies that triggered renal damage in animal models using cyclosporine^{19,52,53}.

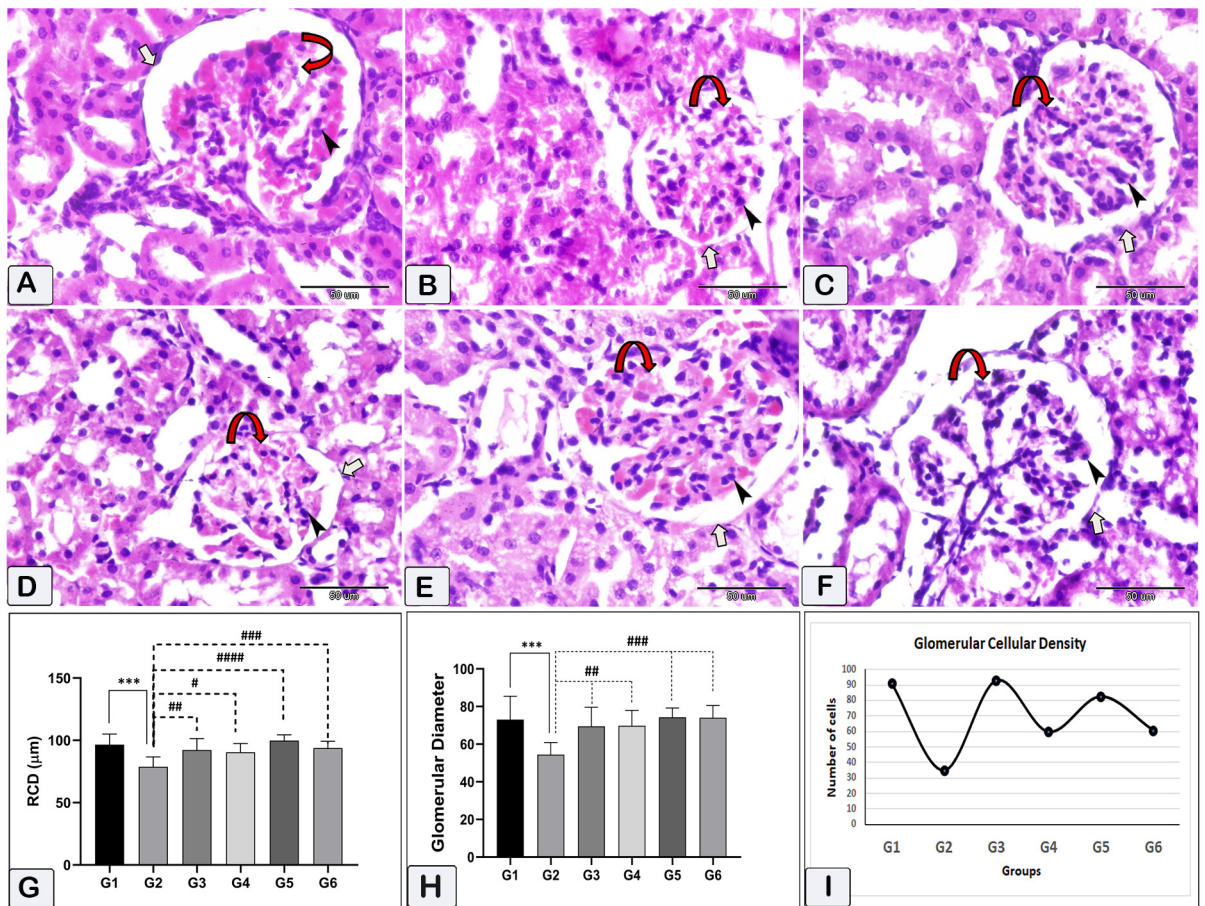


Figure 8. Kidney tissue photomicrographs stained with hematoxylin and eosin (HE). Renal corpuscle diameter, glomerular diameter, and glomerular cell density within the glomeruli were visualized. And estimated. This was achieved by quantifying the number of cell nuclei to assess these parameters. (A) G1, (B) G2, (C) G3, (D) G4, (E) G5, & (F) G6. The curved arrows indicate the location of the glomeruli, black arrowheads indicate the nuclei within the glomeruli, and white arrows indicate the renal corpuscle. G: the renal corpuscle diameter (RCD). (H) the glomerular diameter. (I) the glomerular cell density. *** ($p < 0.001$) Significant difference from control rats. # ($p < 0.05$), ## ($p < 0.01$), ### ($p < 0.001$) & #### ($p < 0.0001$) Significant difference from CsA group. G1 = Control, G2 = CsA-treated rats, G3 = Sitagliptin, G4 = Sitagliptin + CsA, G5 = Hesperidin, G6 = Hesperidin + CsA.

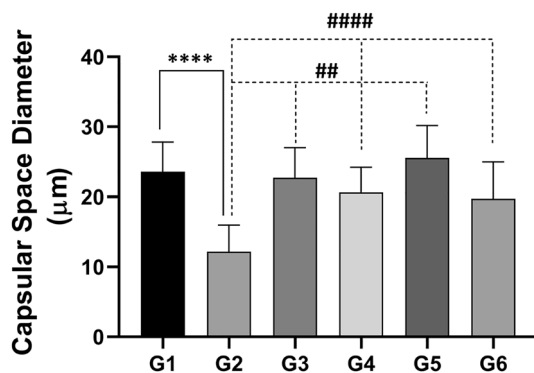


Figure 9. The effect of CsA administration on the capsular space diameter and the potential modification obtained by administering sitagliptin or hesperidin either alone or with CsA. Data represented as mean \pm SEM. *** ($p < 0.001$) Significant difference from control rats. ## ($p < 0.01$), #### ($p < 0.0001$) Significant difference from CsA group. G1 = Control, G2 = CsA-treated rats, G3 = Sitagliptin, G4 = Sitagliptin + CsA, G5 = Hesperidin, G6 = Hesperidin + CsA.

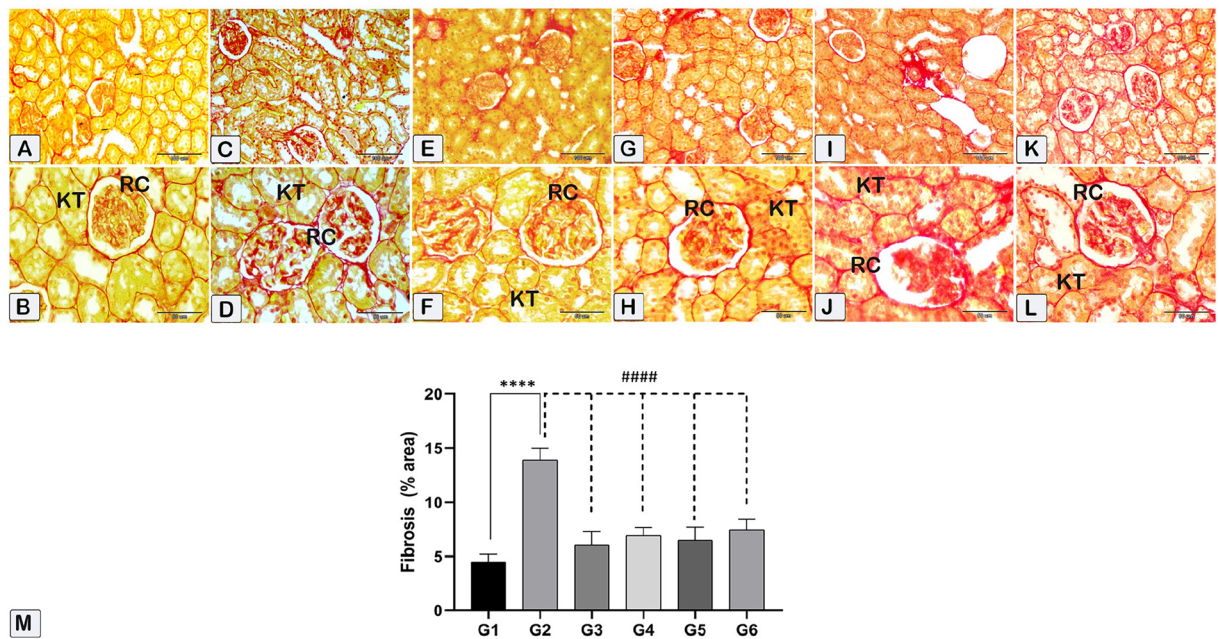


Figure 10. The kidney sections were stained with Sirius Red to measure fibrosis. Red collagenous fibers surround kidney tubules (KT), basement membrane, and renal corpuscles (RC). Histological (A–L) and morphometric assessments of all experimental groups (M) showed that the control group had fewer collagenous fibers than the nephrotoxicity group. However, the fibrosis percentage increased in the nephrotoxicity group and decreased in the treated groups. (A,B) In the control group (G1), kidney tubules and renal corpuscles stained less with collagen fibers than in the toxicity CsA group. (C,D) In the nephrotoxicity group (G2), kidney tubules and renal corpuscles stained more with collagen fibers than in the control group. In G3 (E,F), G4 (G,H), G5 (I,J), and G6 (K,L), a notable decrease in collagen fiber staining was detected in the kidney tubules and renal corpuscles as compared to the nephrotoxicity group. Nevertheless, the observed quantity seemed to be relatively comparable to that observed in the control group. (M) Mean area of morphometric analysis of collagenous fibers % of kidney sections in different groups. **** ($p < 0.0001$) Significant difference from control rats. #### ($p < 0.0001$) Significant difference from CsA group. G1 = Control, G2 = CsA-treated rats, G3 = Sitagliptin, G4 = Sitagliptin + CsA, G5 = Hesperidin, G6 = Hesperidin + CsA.

Cyclosporine caused a significant elevation in serum Cr, BUN, and urinary protein with a significant decrease in serum albumin^{54,55}. Also, cyclosporine injection into rats produced elevations in lipids, and glucose while decreasing albumin and protein levels^{56,57}. The main pathogenesis of CsA-induced hyperglycemia is caused by the direct toxicity of CsA on pancreatic beta cells, which leads to a decrease in insulin production^{58,59}; while insulin resistance plays a minor role in this phenomenon⁶⁰. Our results are consistent with previously mentioned studies, and it was concluded that inhibition of calcineurin might play an important role in the inhibition of the synthesis and release of insulin with hyperglycemia and manifested diabetes⁶¹.

CsA-treated animals showed a spike in MPO activity, indicating renal invasion with inflammatory leukocytes and parenchymal structural derangements⁶². This enzyme is responsible for generating hypochlorous acid during the neutrophil burst reaction, which consequently increases free radical generation and subsequent tissue damage. An increase in the levels of MPO is concomitant with elevated tissue levels of TNF- α , thereby indicating the role of inflammatory cells in organ damage caused by CsA^{8,63}. Daily injections of CsA resulted in significant deterioration of the kidney with elevated serum cystatin C⁶⁴. Our results showed that CsA treatment significantly raised serum levels of Cyst-C and MPO, indicating deteriorated renal function compared with the control rats.

Administration of cyclosporine-A to rats resulted in a dramatic alteration in redox homeostasis, as evidenced by a decrease in tissue antioxidants, GSH, and SOD, and an increase in the levels of the lipid peroxidation marker MDA. These effects of CsA have been attributed to the disruption of mitochondrial oxidative phosphorylation with ROS generation^{2,8}. CsA increases ROS production in several cellular models, decreasing antioxidant levels and inducing lipid peroxidation^{11,65,66}. Also, other studies found that the oxidative parameters in the renal tissues and sera of animals treated with cyclosporine were significantly increased^{67,68}.

The decline in renal tissue SOD activity after CsA administration was also reported in some other studies⁶⁹, and treatment with the SOD mimetic tempol was able to prevent CsA-induced renal dysfunction⁷⁰. In addition, there was decreased serum SOD activity in rats treated with CsA⁷¹. Also, CsA administration to experimental animals resulted in elevated MDA in kidney tissues with lowered CAT activity⁴⁸. Furthermore, CsA produced not only elevated tissue levels of MDA and nitric oxide but also a significant reduction in the tissue levels of several antioxidant enzymes, including CAT, SOD, and GPx. Likewise, CsA led to the accumulation of ROS in the kidney, which directly contributes to renal damage caused by CsA. Growing data suggests that the main mechanism behind CsA-induced nephrotoxicity is apoptosis^{1,72,73}.

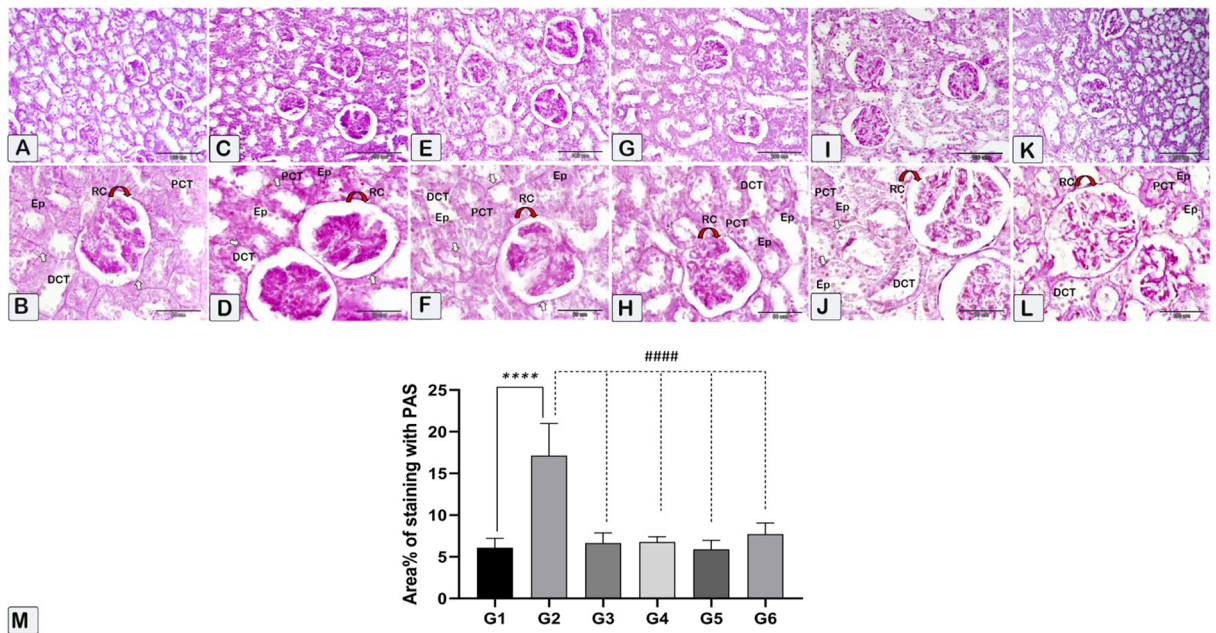


Figure 11. Photographs of paraffin-embedded kidney tissue from the experimental groups are presented. PAS stain was used to color the tissue sections. Brush profits, renal tubule basement membranes, Bowman's capsule, and glomerular tufts of capillaries all show a rich purple color due to the high polysaccharide content of the kidney cortex. (A,B) In the control group (G1), kidney tubules and renal corpuscles stained less than in the toxicity group. (C,D) In the nephrotoxicity group (G2), kidney tubules and renal corpuscles stained more with PAS stain than in the control group. In G3 (E,F), G4 (G,H), G5 (I,J), and G6 (K,L), a notable decrease in staining intensity percentage was detected in the kidney tubules and renal corpuscles as compared to the nephrotoxicity group. (M) Mean area of morphometric analysis of staining intensity % of kidney sections in different groups. G1 = Control, G2 = CsA-treated rats, G3 = Sitagliptin, G4 = Sitagliptin + CsA, G5 = Hesperidin, G6 = Hesperidin + CsA.

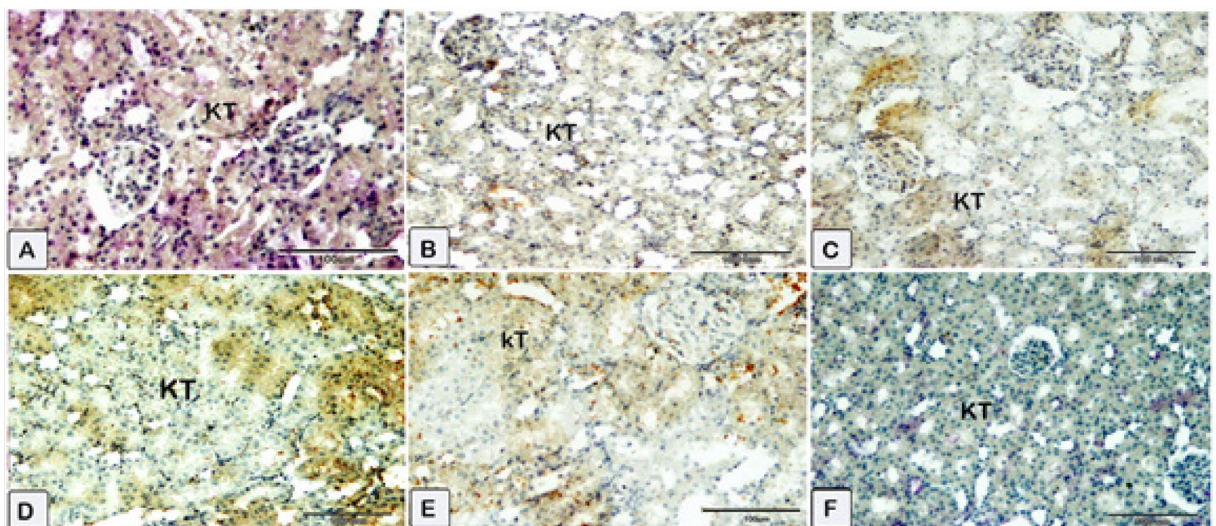


Figure 12. Representative photomicrographs of immunohistochemistry displaying the expression of Nrf2 protein through the application of immunohistochemistry. (A) Sections of the kidney from the control showed average Nrf2 expression (B) Sections of the CsA group showed that renal tubular cells' cytoplasm and nucleus exhibit low levels of Nrf2 expression. (C) Sections of sitagliptin alone, and renal tissues showed near control degree of Nrf2 expression. (D) Sections of the sitagliptin/CsA group showed an average level of Nrf2 expression. (E) Sections of hesperidin alone revealed a similar response as sitagliptin. (F) Sections of the hesperidin/CsA group showed that brown staining was raised in intensity. (A) Control group (G1) (B) CsA group (G2), (C) Sitagliptin group (G3), (D) Sitagliptin + CsA (G4), (E) Hesperidin group (G5), (F) Hesperidin + CsA (G6).

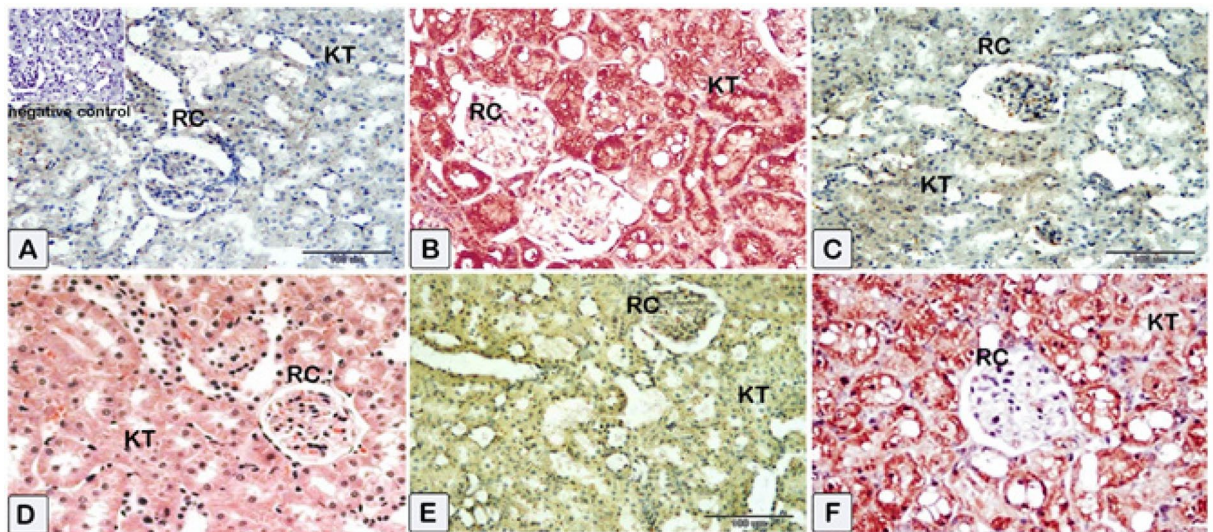


Figure 13. Representative photomicrographs of immunohistochemistry were done to illustrate the mean immunoeexpression levels of Bcl-2-associated X protein (Bax). Results of cytoplasmic Bax positivity in each experimental group (X40) as determined. A substantial positive cytoplasmic Bax reaction was observed in glomerular and tubular cells of the nephrotoxicity group (B), in contrast to the negative reaction observed in the control group (A). The cytoplasmic Bax reaction in glomerular and tubular cells was reduced in rats treated with (C–F). (A) Control group (G1) (B) CsA group (G2), (C) Sitagliptin group (G3), (D) Sitagliptin + CsA (G4), (E) Hesperidin group (G5), (F) Hesperidin + CsA (G6).

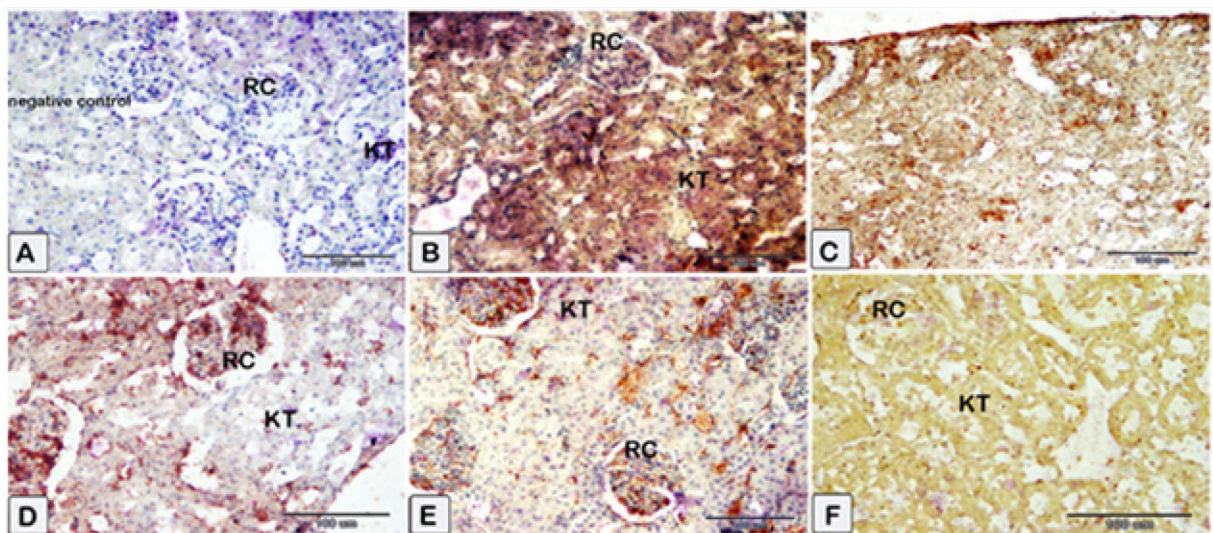


Figure 14. Representative photomicrographs of paraffin sections of kidney tissue acquired from the experimental group, displaying the expression of NF- κ B protein through the application of immunohistochemistry. Group-specific variations in renal NF- κ B protein expression were observed. Reduced levels of the NF- κ B protein are observed control group. The expression of the NF- κ B protein was higher in the nephrotoxicity group than in the control group. Following this, the treated group's expression levels of NF- κ B decreased. (A) Control group (G1) (B) CsA group (G2), (C) Sitagliptin group (G3), (D) Sitagliptin + CsA (G4), (E) Hesperidin group (G5), (F) Hesperidin + CsA (G6).

The glomerular mesangial cells in the kidneys are responsible for the formation of TNF- α , which reduces glomerular blood flow and glomerular filtration rate. Glomerular fibrin deposition because of a decreased glomerular filtration rate results in cellular infiltration and vasoconstriction^{74,75}. As it is evaluated by western blotting, TNF- α expression in the kidney tissues was greatly increased due to CsA administration. In agreement with previous studies, the same finding was determined while investigating the renal effect of CsA⁷⁶. CsA-induced TNF- α higher expression could contribute to the induction of oxidative stress-related apoptosis and renal damage^{77,78}. In addition, it is reported that TNF- α mediates caspase 3/7 activation⁷⁹. CsA-induced renal inflammatory damage is presented by increased TNF- α and lowered adiponectin levels, as well as the aggregation of inflammatory cells with renal vascular congestion⁷⁶.

Rats treated with cyclosporine exhibited enhanced renal inflammation, as evidenced by a significant elevation of pro-inflammatory cytokines such as MCP-1 and TNF- α ⁸⁰. Concurrently, the inflow of activated macrophages and monocytes produces excess pro-inflammatory cytokines, including MCP-1 and TNF- α ; these events cause and maintain increased inflammatory reactions in various renal injury models⁸¹.

Kidneys from rats treated with CsA showed wide capsular space, mesangial lobulation, and shrinking hypercellular glomeruli. The tubules showed diffuse degeneration with focal tubular atrophy and tubular edema, and the stroma showed infiltration by inflammatory cells¹. Tubulointerstitial injury is the most prominent feature of chronic CsA-induced nephropathy, and the major form of cell death is apoptosis⁸². Histologically, there was tubular degeneration, atrophy, basement membrane thickening, and inflammatory cellular infiltration with renal parenchymal changes. Together, are in harmony with the results of previous studies.

Oxidative stress can cause cellular apoptosis through mitochondrial-dependent pathways^{83–85}. High protein expression of Bax with decreased Bcl-2 was revealed in the renal tissue of the CsA-treated animals^{1,73}. Subsequently, this study and other studies by Shihab et al.⁸⁶ and Huang et al.⁸⁷ reported that CsA-induced renal cell apoptosis is associated with an increase in Bax proteins. Increased Bax expression in this study reflects the increased apoptotic death of renal cells. These findings also correlated well with studies done by Temel et al.⁸⁸. In addition, it was shown that via the redox-sensitive Nrf2 pathway, H9c2 cells were protected against apoptosis⁸⁹. On the contrary, there was an increase in Nrf2 mRNA levels in all the CsA-treated groups; Nrf2 is a transcription factor that controls the expression of antioxidant enzymes⁹⁰, and it is very plausible that Nrf2 is produced to decrease the ROS damage induced by the CsA-hypoxic state⁹¹. As we found, administration of CsA increased Bax levels in the kidneys; this was associated with reduced expression of Nrf2. We found that the administration of CsA to rats produced increased oxidative damage, an inflammatory response, and inflammatory cellular infiltration within renal tissue. While the expressions of TNF- α and Bax were induced, the expression of Nrf2 declined significantly. The pro-inflammatory NF- κ B pathway, which plays a critical role in the pathogenesis of CsA nephrotoxicity, was examined to shed light on the molecular processes behind CsA-triggered inflammatory events^{81,92,93}. In line with our findings, NF- κ B protein expression was significantly upregulated following CsA treatment compared to control animals⁹⁴.

We found that hesperidin ameliorated the elevated serum levels of urea and creatinine. Hesperidin exhibited renal protective effects in several previous experiments. Küçükler et al. (2021) found hesperidin treatment considerably alleviated chlorpyrifos-induced renal dysfunction. Also, hesperidin administration relieved the kidney damage induced by paclitaxel and sodium fluoride, lowering blood urea and serum creatinine^{39,95}. Hesperidin treatment significantly decreased the blood glucose, serum insulin, and HOMA-IR values in high-fat diet-induced obese mice⁹⁶. Additionally, oral administration of hesperidin produced a significant amelioration of plasma glucose, insulin, and HbA1c levels compared with the diabetic animals⁹⁷. It was found that hesperidin has potential antihyperglycemic activity in streptozotocin-induced diabetic rats⁹⁸.

Sahu et al. reported that hesperidin ameliorated neutrophil infiltration, as evidenced by a reduction of MPO levels in kidney tissues. Also, Kamel et al.⁹⁹ suggested that hesperidin administration decreased inflammatory cell infiltration in kidney tissues of rats with cisplatin-induced nephrotoxicity. Hesperidin produced a significant reduction of renal MDA and TNF- α , while it led to a significant elevation of GSH, SOD, and CAT⁴⁵. Hesperidin significantly reduced mRNA expression levels of NF- κ B, TNF- α , and Bax, whereas it caused an increase in levels of Nrf2, HO-1, and Bcl-2 in the kidney and liver of paclitaxel-treated rats⁹⁵. Additionally, in anti-tubercular drug-induced hepatic injury, hesperidin reduced the expressions of Bax, NF- κ B, and TNF- α ¹⁰⁰.

Moreover, hesperidin ameliorated the hepatorenal damage caused by acetaminophen, isoniazid, rifampicin, and pyrazinamide by decreasing mRNA levels of Bax and caspase-3^{101,102}. Hesperidin nearly normalized the renal function parameters, inhibited the elevated TNF- α level in the renal tissue, and attenuated the overexpression of caspase-3 and the poor expression of Nrf-2 and HO-1 in methotrexate-induced nephrotoxicity¹⁰³. Hesperidin administration reduced apoptosis, oxidative stress, inflammation, and oxidative DNA damage significantly in sodium arsenite-induced kidney and liver tissues⁴¹. By upregulating Nrf2, hesperidin may help protect cardiomyocytes from the age-related increase in oxidative stress¹⁰⁴. In addition, hesperidin markedly up-regulated the expression of Nrf2 and HO-1 in the liver of diethylnitrosamine /CCl₄-induced rats¹⁰⁵. Furthermore, hesperidin was found to increase Nrf2 protein expression, combating gentamicin-induced nephrotoxicity¹⁰⁶, and diethylnitrosamine/CCl₄-induced renal repercussions¹⁰⁷.

We found that hesperidin administration along with CsA resulted in attenuation of cyclosporine-induced kidney injury. Hesperidin lowered the serum levels of creatinine, urea, glucose, Cyst-C, and MPO, while elevating the serum albumin; this is in line with other previous studies. Our results showed that hesperidin antagonized oxidative stress by decreasing MDA levels in kidney tissue with elevated GSH levels. Additionally, the antioxidant stress enzymes, which represent the defense mechanisms of renal SOD and CAT, were maintained near normal by hesperidin treatment. Hesperidin attenuated CsA-induced overexpression of TNF- α in kidney tissues, indicating its significant anti-inflammatory effect.

In agreement with other studies, we found hesperidin to downregulate the expression of Bax and NF- κ B and upregulate the expression of Nrf-2. These findings coincide with other findings that hesperidin has cytoprotective, antioxidant, and antiapoptotic properties. It is noteworthy to mention that hesperidin ameliorated the pathological changes inhibiting the cellular infiltration within renal tissue induced by CsA and preserved the glomerular, tubular, and interstitial kidney structure, as was found previously in the mentioned studies.

Sitagliptin impedes the enzyme DPP-4, which is expressed in many tissues, including the kidneys¹⁰⁸. DPP-4 inhibitors increase the circulating GLP-1 concentrations and improve glucose metabolism with antidiabetic effects¹⁰⁹. Stimulation of the GLP-1R in blood vessels results in the relaxation of smooth muscle and increased renal blood flow¹¹⁰. In the normal kidney, stimulation of GLP-1R by GLP-1 results in natriuresis and water loss¹¹¹. Treatment with DPP-4 inhibitors, which increase GLP-1 levels, has been shown to exert numerous renoprotective effects. These effects include a reduction in blood glucose and lipid levels, inhibition of inflammation and

oxidative stress, amelioration of mesangial expansion, and an elevation of the glomerular filtration rate (GFR)¹¹². Several mechanisms might be responsible for the renoprotective effects of sitagliptin against renal I/R such as the restoration of normoglycemia¹¹³.

Our results are in harmony with other studies that reported the capability of sitagliptin to improve kidney function and attenuate the histopathological changes in different experimental models such as diabetic nephropathy¹¹⁴, ischemia–reperfusion injury³⁴, gentamicin nephrotoxicity¹¹⁵, and cisplatin-induced nephrotoxicity in mice¹¹⁶. In agreement with previous studies, sitagliptin produced a significant decrease in serum urea, creatinine, MPO, and cyst-C levels while preserving serum albumin compared to the nephrotoxicity group of rats.

Levels of MPO were found to be significantly higher in rats treated with CsA compared to the control group; a significant decrease in this parameter was observed in the group administered with CsA and sitagliptin or CsA and hesperidin. Catalase and SOD levels in the renal tissues were markedly decreased in the CsA-received group compared to the control animals. However, sitagliptin or hesperidin use together with CsA caused a significant increase in these antioxidant enzymes. Other studies postulated and reported the same findings¹¹⁷.

Sitagliptin exerted a renoprotective effect against ischemia–reperfusion injury through attenuating oxidative stress¹¹⁸. Moreover, sitagliptin improved cardiac mitochondrial dysfunction¹¹⁹ and attenuated brain mitochondrial dysfunction¹²⁰ in insulin-resistant rats¹¹⁵. Oxidative stress markers such as MDA, NO, and advanced protein oxidation product concentrations were increased in the two kidney and one clip (2K1C) rats and were also normalized by sitagliptin treatment¹²¹.

Co-administration of Sitagliptin to gentamicin-administered rats significantly decreased the serum BUN and creatinine levels and the urinary excretion of total protein levels. Also, sitagliptin significantly restored the levels of GSH, GPx, SOD, CAT, and MDA compared to the gentamicin group¹¹⁵. Moreover, sitagliptin treatment significantly suppressed lipid peroxidation in methotrexate-intoxicated rats and significantly increased renal SOD, GPx, and catalase activities³². Our findings were consistent with previous work that demonstrated how sitagliptin decreased oxidative stress in the ovalbumin-induced asthma model by lowering MDA concentration and reverting SOD and GSH levels to normal¹²². Therefore, sitagliptin might reduce oxidative burden by decreasing reactive oxygen species (ROS) generation⁵⁵.

Sitagliptin, according to Fan et al.¹²³, inhibited the expression of IL-6 and TNF- α . In a rat model of heart failure, sitagliptin decreased inflammation and fibrosis since its treatment reversed the increase in TNF- α and IL-6 in the myocardium¹²⁴. In rats with chronic cerebral hypoperfusion, sitagliptin reduced brain damage and cognitive impairment by reducing oxidative stress and the inflammatory response. Also, treatment with sitagliptin decreased the mRNA expressions of TNF- α , NF- κ B, and Bax¹²⁵. Moreover, sitagliptin was found to attenuate the renal expressions of TNF- α , and NF- κ B in renal ischemia/reperfusion³⁴. Additionally, sitagliptin reduced the expressions of Bax, TNF- α and NF- κ B in transient cerebral ischemia/reperfusion injury in diabetic rats¹²⁶.

Sitagliptin treatment with CsA significantly inhibited the decrease in Nrf-2 levels in the kidneys. Sitagliptin treatment in mice upregulates the Nrf2 signaling pathway and promotes Nrf2 nuclear translocation. Also, under the action of sitagliptin, Nrf2 migrated to the nucleus and inhibited autophagy, thereby reducing inflammation¹²⁷. What's more, sitagliptin prevented gentamicin-induced renal tubular apoptosis by exhibiting a significant decrease in caspase-3 and Bax immunoreactive cells in kidney Sections¹¹⁵.

Histologically, in streptozotocin-induced diabetic mice, there was notable renal tubular dilatation, mesangial matrix deposition, and tubulointerstitial fibrosis when compared with control mice. However, sitagliptin administration significantly ameliorated these morphologic injuries and tubular changes¹²⁸. Sitagliptin reversed and preserved renal histostructure in different models of acute kidney injuries as well^{33,112,115,116}.

Our findings demonstrated sitagliptin's capacity to combat cyclosporine-induced nephrotoxicity. When compared to CsA-treated rats, the treatment of sitagliptin along with CsA resulted in the normalization of serum creatinine and blood urea, as well as near-normal serum albumin levels, decreased glucose levels, and decreased Cyst-C levels. The treatment of sitagliptin dramatically reduced MPO, an indication of neutrophil infiltration and activity in the kidneys. Consistent with other earlier research, sitagliptin maintained the kidney's oxidant/antioxidant balance, as seen by lipid peroxidation inhibition, higher GSH levels, and improved SOD and CAT activity. Histopathological results of this study have shown that renal damage was successfully mitigated when animals were treated with sitagliptin before and concurrently with CsA administration. In agreement with other research, sitagliptin was found to downregulate the expression of inflammatory cytokines such as TNF- α . Also, immunohistochemical examination showed sitagliptin's ability to impede the overexpression of Bax, which is considered an indicator of cellular apoptosis, and NF- κ B, which is considered an inflammatory mediator, while on the contrary, sitagliptin upregulated the expression of Nrf-2, enhancing the antioxidant mechanisms of renal tissue.

It's noteworthy that sitagliptin was able to preserve the structure and function of the renal tissue in rats administered CsA owing to its anti-inflammatory, antioxidant, and antiapoptotic aspects. Hesperidin and sitagliptin both exhibited almost similar effects; however, findings from biochemical, histological, and immunohistochemical studies indicated that sitagliptin would be more advantageous in avoiding kidney damage induced by CsA.

Methods

Animals

Mature male Wistar albino rats (n = 36), weighing 200 \pm 20 g, were utilized in this investigation. They were purchased from the Animal House of the Faculty of Medicine at Assiut University, Assiut, Egypt. The animals were acclimated to laboratory conditions for 10 days, with a 12-h light and 12-h dark cycle, standard humidity, and temperature, to ensure they adapted to their new environment. Animals had free access to food and water. All experimental procedures and animal care in this study were monitored and approved by the National Research Council's Guide for the Care and Use of Laboratory Animals and permitted by the Research Ethics Committee, Faculty of Pharmacy, Beni-Suef University (BSU-IACUC) (Number: 022-360).

Drug and chemicals

Cyclosporine (CAS No.: 59865-13-3), Sitagliptin (CAS No.: 486460-32-6), and Hesperidin (CAS No.: 520-26-3) were purchased from Sigma-Aldrich (St. Louis, MO). All other chemicals used for the investigation were of analytical grade.

Experimental design and animal group

The animals in the present experiment were allocated into 6 groups (n = 6). Group 1 (G1): Control rats were administered to the vehicle for 14 days. Group 2 (G2): Rats received CsA (20 mg/kg/day, i.p. for 7 days)^{1,129}. It was injected as a solution in normal saline for 7 days. Group 3 (G3): Rats received sitagliptin orally for 14 days at a dose of 10 mg/kg/day dissolved in saline^{130,131}. Group 4 (G4): Rats received both CsA and sitagliptin regimens, as previously mentioned. Sitagliptin was administered 7 days before starting CsA, and then both drugs were given concomitantly for another 7 days. Group 5 (G5): Rats were given oral hesperidin (200 mg/kg/day) for 14 days^{39,95}. Hesperidin was prepared in normal saline. Group 6 (G6): Rats received both CsA and hesperidin treatments as per the previously mentioned dose regimen. Hesperidin was administered 7 days before CsA, and for another 7 days, they were administered concurrently (Fig. 15).

Blood samples were taken under intraperitoneal pentobarbital anesthesia (35 mg/kg) from the retro-orbital plexus. Blood samples were centrifuged at 10,000 RPM for 5 min after being left for half an hour, then stored at -20°C until analysis. After the animals were sacrificed, the kidneys were promptly removed, and three times rinsed in ice-cooled normal saline. Each left kidney was divided into two portions; one was used for preparing kidney homogenates (10% w/v), and 500 mg of each kidney tissue was homogenized in 5 mL phosphate buffer (0.1 M, pH 7.4). The homogenates were then kept frozen at -20°C for the subsequent biochemical assay. The second portion of the left kidney was homogenized in RIPA buffer and utilized for western blot analysis of kidney tissue TNF- α protein expression. The right kidneys were fixed in 10% neutral buffered formalin for the assessment of histopathological renal damage and to perform immunohistochemical investigations.

Biochemical analysis

Serum level of urea and creatinine

The serum levels of urea and creatinine were determined using available commercial kits [COD 11,516 (urea), COD 11,734 (creatinine), BioSystems S.A. Costa Brava, Barcelona, Spain] and according to the instructions of the manufacturer.

Serum albumin and cystatin C

By using a commercially available ELISA kit (Cat. No. BSIS02-I), the serum level of albumin was measured following the instructions of the manufacturer (SPINREACT, Santa Coloma, Spain). The serum level of cystatin-C was estimated using a commercially available Rat Cys-C ELISA kit (Catalog No.: E-EL-R0304) and following the manufacturer's instructions (Elabscience Biotechnology Co., Ltd., Wuhan, Hubei, China).

Determination of serum myeloperoxidase (MPO)

According to the manufacturer's instructions, serum MPO was determined using the available ELISA kit from FineTest Biotech Inc., US (Cat. No.: ER0142).

Blood glucose level

It was performed using an available commercial kit (Cat. No. BSIS17-1), and the serum level of albumin was measured following the instructions of the manufacturer (SPINREACT, Santa Coloma, Spain).

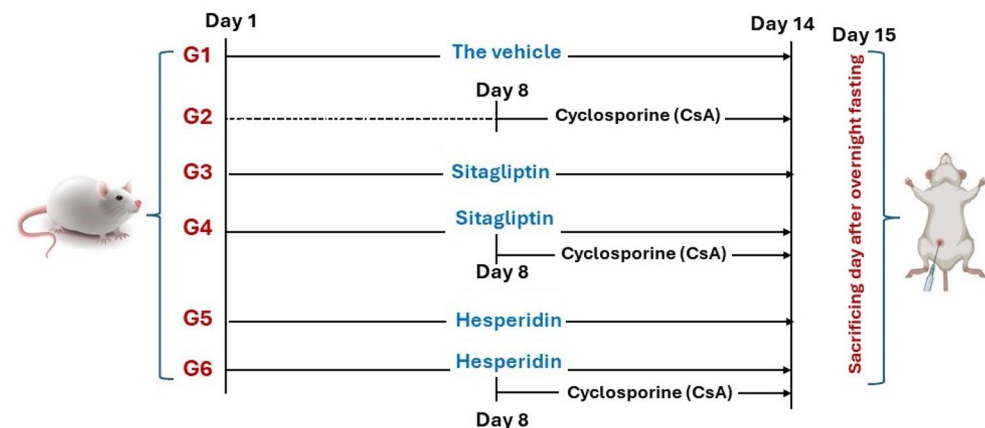


Figure 15. The schematic representation of the experimental design including drugs and the duration of administration. G1: Control group, G2: CsA group, G3: Sitagliptin group, G4: Sitagliptin + CsA group, G5: Hesperidin group and G6: Hesperidin + CsA group.

Determination of tissue malondialdehyde (MDA)

The renal tissue level of MDA was estimated as an indicator of lipid peroxidation. This was performed according to instructions and steps described in the colorimetric method described by Ohkawa et al.¹³² and by using a commercially available kit (CAT. No. MD 2529) (Biodiagnostic, Giza, Egypt).

Determination of glutathione reduced (GSH)

According to the method described by Beutler et al.¹³³ the GSH level in the kidney tissue was using a commercially available kit (CAT. No.: GR 2511) (Biodiagnostic, Giza, Egypt). The method is based on the reduction of 5,5'-dithiobis (2-nitrobenzoic acid) (DTNB) with glutathione (GSH) to produce a yellow compound. The reduced chromogen is directly proportional to GSH concentration, and its absorbance can be measured at 405 nm.

Determination of catalase (CAT) activity

This was done by the utilization of an available colorimetric kit (CAT. No.: CA 2517, Biodiagnostic, Giza, Egypt) and a method described by Aebi¹³⁴.

The SOD activity

The principle of the total SOD activity method is based, briefly, on the inhibition of nitro blue tetrazolium (NBT) reduction by the generated xanthine/xanthine oxidase system¹³⁵. The activity was assessed in the ethanol phase of the serum after the addition of 1.0 ml of the ethanol/chloroform mixture (5/3, v/v) to the same volume of centrifuge. One unit of SOD was defined as the enzyme amount causing 50% inhibition in the NBT reduction rate. The SOD activity was expressed as a U/g protein. The assay was performed using a commercially available colorimetric kit (CAT. No. SD 2521, Biodiagnostic, Giza, Egypt).

Western blot analysis for renal TNF- α

To achieve a clear supernatant, tissue samples were centrifuged after being homogenized in RIPA buffer. The total protein content was determined using the Bradford reagent. SDS-PAGE was used to isolate 30 μ g of protein per gel lane, and the protein was then transferred to a PVDF membrane. The membranes were then treated with primary antibodies against TNF-alpha antibody after being blocked in Tris-buffered saline with Tween 20 (TBST) containing 5% non-fat milk powder (Novus Biologicals USA). By ensuring that protein loading is uniform throughout the gel, the housekeeping protein β -actin was utilized as a loading control to normalize the quantities of protein observed. The membranes were TBST-washed before being incubated for an hour with horseradish peroxidase-conjugated secondary antibodies from Novus Biologicals in Littleton, Colorado, USA. An improved chemiluminescence kit was used to find immuno-labeling (BioRad, Hercules, CA). Finally, we will utilize ImageJ to scan the acquired blots and quantify band intensities (NIH, Bethesda, Maryland, USA).

Histopathological examination

The obtained kidney specimens from each rat were fixed in the following fixative: 40 mL paraformaldehyde, 125 mL phosphate buffer (0.2 M, pH 7.4), 25% freshly made, 37.5 mL saturated picric acid, 0.5 mg calcium chloride, 1.25 mL glutaraldehyde 25%, and distilled water was added up to 250 mL. The specimens were fixed using Wrobel–Moustafa fixative for 24 h. The fixed samples were thoroughly washed with 70% ethanol three times over 24 h. Following cleaning, samples were encased in paraffin wax. Using a Reichert Leica RM2125 Microtome, sections were cut between 5 and 7 μ m.

Hematoxylin and eosin stain was used to stain paraffin representative sections for general histological study and scoring (H&E). Other sections were stained with Periodic Acid-Schiff (PAS) stain to evaluate the glomerular basement membrane thickening and damage. Additionally, Sirius red stain was used to investigate fibrosis (Red color) in the kidney section of various groups^{136,137}.

Sirius Red staining was performed to determine the percentage fibrosis area: incubating slides in 0.1% Sirius Red F3B for 1 h, washing twice in acidified water, dehydrating thrice in 100% ethanol, and then clearing in xylene. Interstitial fibrosis is commonly measured by histology. Sirius Red staining is specific for collagen type I and III fibrils¹³⁸. Sirius red fibrosis was quantified using image analysis to determine the percentage fibrosis area¹³⁶.

According to the method published by Abd-Eldayem et al.¹³⁹ we used Image J to calculate the area % of staining intensity of PAS stain in images from various experimental groups. Launch the image editing software J Fiji and open each picture separately. Click “type” and then “8-bit” to convert the image in the image column to an 8-bit image; click “analyze column” and choose the measurement; click “okay” after verifying the area and area fraction; click “image” and click “adjust” and then click “threshold” You can change the backdrop color to white, red, or black using the drop-down choices. Adjust the top slider until the foreground of the image is fully red to perform a threshold. As much as possible, maintain a uniform stain. To finish, hit the “Apply” button.

Immunohistochemical determination of Bax and Nrf-2 and NF- κ B

Paraffin tissue sections were rehydrated and deparaffinized using ethanol and double-distilled water. Antigen retrieval was performed as slides were completely submerged in excess amounts of a pre-heated antigen retrieval solution and microwaved until boiling. Continuous boiling was maintained for at least 15 min. After boiling, we washed slides four times in buffer, followed by the application of block, and then incubated for 5 min at room temperature and away from light. Then, they were washed once in the buffer. After washing, the primary antibodies for Bax [Bax antibody (Cat. No. GTX32465), Gene Tex, USA], Nrf2 [NRF2 antibody (Cat. No. GTX55732), Gene Tex, USA], and NF- κ B [NF κ B p105 (phospho Ser927) antibody, (Cat. No. GTX32222), Gene Tex, USA] were applied at a dilution of 1/100 and incubated overnight. Washing was done four times in the buffer, followed

by placing the biotinylated link antibody, and then left at room temperature for 15–20 min. After washing four times in the buffer, streptavidin/HRP was applied and then left at room temperature for 20 min. Following four times rinsing in the buffer, DAB chromogen was mixed thoroughly and then applied to slides for 5 min. After rinsing once in distilled water, the DAB Chromogen/Substrate was applied for 5 min before rinsing and this was followed by counterstaining. The coverslip was placed for each slide using DI followed by examination. We utilized a Leitz Dialux 20 microscope and a Canon PowerShot A95 digital camera to evaluate immunohistochemistry staining.

Statistical analysis

Statistical assessment was conducted using GraphPad Prism 8 software (One-way ANOVA with a post-hoc Tukey's correction) and the SPSS program (version 17) (One-way ANOVA, followed by the Scheffe and Duncan test). To identify any significant differences between the pre-treatment and treatment groups, a T-test was applied. A p -value < 0.05 was deemed significant.

Ethical approval and consent to participate

The study's protocol was approved by the Faculty of Pharmacy, Beni-Suef University's Ethics Committee for Animal Experimentation (BSU-IACUC) (Number: 022-360). All methods were performed in accordance with the relevant guidelines and regulations. The study is also presented in accordance with ARRIVE guidelines.

Data availability

The datasets generated and/or analyzed during the current study are available from the corresponding author upon reasonable request.

Received: 10 December 2023; Accepted: 16 March 2024

Published online: 28 March 2024

References

- Ateyya, H. Amelioration of cyclosporine induced nephrotoxicity by dipeptidyl peptidase inhibitor vildagliptin. *Int. Immunopharmacol.* **28**, 571–577 (2015).
- Wu, Q. *et al.* Mechanism of cyclosporine A nephrotoxicity: Oxidative stress, autophagy, and signalings. *Food Chem. Toxicol.* **118**, 889–907 (2018).
- El-Sheikh, A. A. K., Morsy, M. A. & Abdel-latif, R. G. Modulation of eNOS/iNOS by nebulivol protects against cyclosporine A-mediated nephrotoxicity through targeting inflammatory and apoptotic pathways. *Environ. Toxicol. Pharmacol.* **69**, 26–35 (2019).
- O'Connell, S., Slattery, C., Ryan, M. P. & McMorrow, T. Identification of novel indicators of cyclosporine A nephrotoxicity in a CD-1 mouse model. *Toxicol. Appl. Pharmacol.* **252**, 201–210 (2011).
- Hye, E. Y. & Chul, W. Y. Established and newly proposed mechanisms of chronic cyclosporine nephropathy. *Korean J. Intern. Med.* **24**, 81–92 (2009).
- Josephine, A. *et al.* Beneficial effects of sulfated polysaccharides from *Sargassum wightii* against mitochondrial alterations induced by Cyclosporine A in rat kidney. *Mol. Nutr. Food Res.* **51**, 1413–1422 (2007).
- O'Connell, S., Tuite, N., Slattery, C., Ryan, M. P. & McMorrow, T. Cyclosporine A-induced oxidative stress in human renal mesangial cells: A role for ERK 1/2 MAPK signaling. *Toxicol. Sci.* **126**, 101–113 (2012).
- Vangaveti, S., Das, P. & Kumar, V. L. Metformin and silymarin afford protection in cyclosporine A induced hepatorenal toxicity in rat by modulating redox status and inflammation. *J. Biochem. Mol. Toxicol.* **35**, e22614 (2021).
- Joshi, S., Peck, A. B. & Khan, S. R. NADPH oxidase as a therapeutic target for oxalate induced injury in kidneys. *Oxid. Med. Cell. Longev.* **2013**, (2013).
- El-Naga, R. N. Pre-treatment with cardamonin protects against cisplatin-induced nephrotoxicity in rats: Impact on NOX-1, inflammation and apoptosis. *Toxicol. Appl. Pharmacol.* **274**, 87–95 (2014).
- de Arriba, G., Calvino, M., Benito, S. & Parra, T. Cyclosporine A-induced apoptosis in renal tubular cells is related to oxidative damage and mitochondrial fission. *Toxicol. Lett.* **218**, 30–38 (2013).
- Lee, S. *et al.* Protective effect of COMP-angiopoietin-1 on cyclosporine-induced renal injury in mice. *Nephrol. Dial. Transplant* **23**, 2784–2794 (2008).
- Nam, H. K. *et al.* Rosuvastatin attenuates inflammation, apoptosis and fibrosis in a rat model of cyclosporine-induced nephropathy. *Am. J. Nephrol.* **37**, 7–15 (2013).
- Carlos, C. P., Sonehara, N. M., Oliani, S. M. & Burdman, E. A. Predictive usefulness of urinary biomarkers for the identification of cyclosporine A-induced nephrotoxicity in a rat model. *PLoS ONE* **9**, e103660 (2014).
- M, A. *et al.* TNF is an essential mediator in lupus nephritis | Request PDF. *Arthritis Rheum* 3418–3419 https://www.researchgate.net/publication/230556983_TNF_is_an_essential_mediator_in_lupus_nephritis (2002).
- Ibrahim, S. R. M. *et al.* Natural reno-protective agents against cyclosporine A-induced nephrotoxicity: An overview. *Molecules* **27**, 7771 (2022).
- Wardyn, J. D., Ponsford, A. H. & Sanderson, C. M. Dissecting molecular cross-talk between Nrf2 and NF- κ B response pathways. *Biochem. Soc. Trans.* **43**, 621–626 (2015).
- He, M. *et al.* Activation of the Nrf2/HO-1 antioxidant pathway contributes to the protective effects of Lycium barbarum polysaccharides in the rodent retina after ischemia-reperfusion-induced damage. *PLoS ONE* **9**, e84800 (2014).
- Nouri, A. *et al.* Ferulic acid prevents cyclosporine-induced nephrotoxicity in rats through exerting anti-oxidant and anti-inflammatory effects via activation of Nrf2/HO-1 signaling and suppression of NF- κ B/TNF- α axis. *Naunyn. Schmiedebergs. Arch. Pharmacol.* **395**, 387–395 (2022).
- Lawrence, T. The nuclear factor NF- κ B pathway in inflammation. *Cold Spring Harb. Perspect. Biol.* **1**, a001651 (2009).
- Magendiramani, V. *et al.* S-allylcysteine attenuates renal injury by altering the expressions of iNOS and matrix metallo proteinase-2 during cyclosporine-induced nephrotoxicity in Wistar rats. *J. Appl. Toxicol.* **29**, 522–530 (2009).
- Penno, G., Garofolo, M. & Del Prato, S. Dipeptidyl peptidase-4 inhibition in chronic kidney disease and potential for protection against diabetes-related renal injury. *Nutr. Metab. Cardiovasc. Dis.* **26**, 361–373 (2016).
- Nicotera, R. *et al.* Antiproteinuric effect of DPP-IV inhibitors in diabetic and non-diabetic kidney diseases. *Pharmacol. Res.* **159**, 105019 (2020).

24. Arjona Ferreira, J. C. *et al.* Efficacy and safety of sitagliptin versus glipizide in patients with type 2 diabetes and moderate-to-severe chronic renal insufficiency. *Diabetes Care* **36**, 1067–1073 (2013).
25. Plosker, G. L. Sitagliptin: A review of its use in patients with type 2 diabetes mellitus. *Drugs* **74**, 223–242 (2014).
26. Mega, C., Teixeira-De-Lemos, E., Fernandes, R. & Reis, F. Renoprotective effects of the dipeptidyl peptidase-4 inhibitor sitagliptin: A review in type 2 diabetes. *J. Diabetes Res.* **2017**, (2017).
27. Al-Qabbaa, S. M. *et al.* Sitagliptin mitigates diabetic nephropathy in a rat model of streptozotocin-induced type 2 diabetes: Possible role of PTP1B/JAK-STAT pathway. *Int. J. Mol. Sci.* **24**, 6532 (2023).
28. Jo, C. H., Kim, S., Park, J. S. & Kim, G. H. Anti-inflammatory action of sitagliptin and linagliptin in doxorubicin nephropathy. *Kidney Blood Press. Res.* **43**, 987–999 (2018).
29. Wang, D. *et al.* Sitagliptin ameliorates diabetic nephropathy by blocking TGF- β 1/Smad signaling pathway. *Int. J. Mol. Med.* **41**, 2784–2792 (2018).
30. Mohamed, R. H. *et al.* Sitagliptin's renoprotective effect in a diabetic nephropathy model in rats: The potential role of PI3K/AKT pathway. *Fundam. Clin. Pharmacol.* **36**, 324–337 (2022).
31. Shi, W., Zhang, D., Wang, L., Sreeharsha, N. & Ning, Y. Curcumin synergistically potentiates the protective effect of sitagliptin against chronic deltamethrin nephrotoxicity in rats: Impact on pro-inflammatory cytokines and Nrf2/Ho-1 pathway. *J. Biochem. Mol. Toxicol.* **33**, e22386 (2019).
32. Afkhami Fard, L. *et al.* Protective effects of sitagliptin on methotrexate-induced nephrotoxicity in rats. *J. Environ. Sci. Heal. Part C Toxicol. Carcinog.* **41**, 22–35. <https://doi.org/10.1080/26896583.2023.2186683> (2023).
33. Al Suleimani, Y. M. *et al.* The effect of the dipeptidyl peptidase-4 inhibitor sitagliptin on gentamicin nephrotoxicity in mice. *Biomed. Pharmacother.* **97**, 1102–1108 (2018).
34. Chen, Y. T. *et al.* Exendin-4 and sitagliptin protect kidney from ischemia-reperfusion injury through suppressing oxidative stress and inflammatory reaction. *J. Transl. Med.* **11**, 1–9 (2013).
35. Chang, M. W. *et al.* Sitagliptin protects rat kidneys from acute ischemia-reperfusion injury via upregulation of GLP-1 and GLP-1 receptors. *Acta Pharmacol. Sin.* **36**, 119–130 (2015).
36. Abdelrahman, A. M. *et al.* The renoprotective effect of the dipeptidyl peptidase-4 inhibitor sitagliptin on adenine-induced kidney disease in rats. *Biomed. Pharmacother.* **110**, 667–676 (2019).
37. Pyrzynska, K. Hesperidin: A review on extraction methods, stability and biological activities. *Nutrients* **14**, 2387 (2022).
38. Karacaer, C. *et al.* The protective effects of hesperidin pretreatment on kidney and remote organs against renal ischemia-reperfusion injury. *Eur. Rev. Med. Pharmacol. Sci.* **27**, 2808–2814 (2023).
39. Caglayan, C., Kandemir, F. M., Darendelioglu, E., Küçükler, S. & Ayna, A. Hesperidin protects liver and kidney against sodium fluoride-induced toxicity through anti-apoptotic and anti-autophagic mechanisms. *Life Sci.* **281**, 119730 (2021).
40. Varışlı, B. *et al.* Hesperidin attenuates oxidative stress, inflammation, apoptosis, and cardiac dysfunction in sodium fluoride-induced cardiotoxicity in rats. *Cardiovasc. Toxicol.* **22**, 727–735 (2022).
41. Turk, E. *et al.* Protective effect of hesperidin on sodium arsenite-induced nephrotoxicity and hepatotoxicity in rats. *Biol. Trace Elem. Res.* **189**, 95–108 (2019).
42. Elhelaly, A. E. *et al.* Protective effects of hesperidin and diosmin against acrylamide-induced liver, kidney, and brain oxidative damage in rats. *Environ. Sci. Pollut. Res. Int.* **26**, 35151–35162 (2019).
43. Küçükler, S., Çomaklı, S., Özdemir, S., Çağlayan, C. & Kandemir, F. M. Hesperidin protects against the chlorpyrifos-induced chronic hepato-renal toxicity in rats associated with oxidative stress, inflammation, apoptosis, autophagy, and up-regulation of PARP-1/VEGF. *Environ. Toxicol.* **36**, 1600–1617 (2021).
44. Hassan, N. H., Yousef, D. M. & Alsemeh, A. E. Hesperidin protects against aluminum-induced renal injury in rats via modulating MMP-9 and apoptosis: Biochemical, histological, and ultrastructural study. *Environ. Sci. Pollut. Res. Int.* **30**, 36208–36227 (2023).
45. Kaltalioglu, K. & Coskun-Cevher, S. Potential of morin and hesperidin in the prevention of cisplatin-induced nephrotoxicity. *Ren. Fail.* **38**, 1291–1299 (2016).
46. Gelen, V. *et al.* The protective effects of hesperidin and curcumin on 5-fluorouracil-induced nephrotoxicity in mice. *Environ. Sci. Pollut. Res. Int.* **28**, 47046–47055 (2021).
47. Mas-Capdevila, A. *et al.* Effect of hesperidin on cardiovascular disease risk factors: The role of intestinal microbiota on hesperidin bioavailability. *Nutrients* **12**, 1488 (2020).
48. Gokce, M. *et al.* Cilostazol and diltiazem attenuate cyclosporine-induced nephrotoxicity in rats. *Transplant. Proc.* **44**, 1738–1742 (2012).
49. Cattaneo, D., Perico, N., Gaspari, F. & Remuzzi, G. Nephrotoxic aspects of cyclosporine. *Transplant. Proc.* **36**, S234–S239 (2004).
50. Myers, B. D., Ross, J., Newton, L., Luetscher, J. & Perlroth, M. Cyclosporine-associated chronic nephropathy. *N. Engl. J. Med.* **311**, 699–705 (1984).
51. Yeboah, M. M. *et al.* The epoxyicosatrienoic acid analog PVPA ameliorates cyclosporine-induced hypertension and renal injury in rats. *Am. J. Physiol. Renal Physiol.* **311**, F576–F585 (2016).
52. Adekunle, I. A., Imafidon, C. E., Oladele, A. A. & Ayoka, A. O. Ginger polyphenols attenuate cyclosporine-induced disturbances in kidney function: Potential application in adjuvant transplant therapy. *Pathophysiol. Off. J. Int. Soc. Pathophysiol.* **25**, 101–115 (2018).
53. Hashemi, S. R., Arab, H. A., Seifi, B. & Muhammadnejad, S. A comparison effects of l-citrulline and l-arginine against cyclosporine-induced blood pressure and biochemical changes in the rats. *Hipertens. y riesgo Vasc.* **38**, 170–177 (2021).
54. Ghafil, F. A., Kadhim, S. A. A., Majeed, S., Qassam, H. & Hadi, N. R. Nephroprotective effects of candesartan cilexetil against cyclosporine A-induced nephrotoxicity in a rat model. *J. Med. Life* **15**, 1553–1562 (2022).
55. El-Kashef, D. H. & Serrya, M. S. Sitagliptin ameliorates thioacetamide-induced acute liver injury via modulating TLR4/NF-KB signaling pathway in mice. *Life Sci.* **228**, 266–273 (2019).
56. Xiang, Y. *et al.* L-carnitine protects against cyclosporine-induced pancreatic and renal injury in rats. *Transplant. Proc.* **45**, 3127–3134 (2013).
57. Aziz, M. M., Eid, N. I., Nada, A. S., Amin, N. E. D. & Ain-Shoka, A. A. Possible protective effect of the algae spirulina against nephrotoxicity induced by cyclosporine A and/or gamma radiation in rats. *Environ. Sci. Pollut. Res. Int.* **25**, 9060–9070 (2018).
58. Chung, B. H. *et al.* Rosiglitazone protects against cyclosporine-induced pancreatic and renal injury in rats. *Am. J. Transplant.* **5**, 1856–1867 (2005).
59. Lim, S. W. *et al.* Oral administration of ginseng ameliorates cyclosporine-induced pancreatic injury in an experimental mouse model. *PLoS ONE* **8**, e72685 (2013).
60. Nam, J. H. *et al.* beta-Cell dysfunction rather than insulin resistance is the main contributing factor for the development of postrenal transplantation diabetes mellitus. *Transplantation* **71**, 1417–1423 (2001).
61. Hecking, M., Sharif, A., Eller, K. & Jenssen, T. Management of post-transplant diabetes: Immunosuppression, early prevention, and novel antidiabetics. *Transpl. Int.* **34**, 27 (2021).
62. Guo, S. X. *et al.* Effects of hydrogen-rich saline on early acute kidney injury in severely burned rats by suppressing oxidative stress induced apoptosis and inflammation. *J. Transl. Med.* **13**, 1–15 (2015).
63. Biswas, S. K. Does the interdependence between oxidative stress and inflammation explain the antioxidant paradox? *Oxid. Med. Cell. Longev.* **2016**, (2016).

64. Al-Rabia, M. W. *et al.* 2-Methoxyestradiol TPGS micelles attenuate cyclosporine A-induced nephrotoxicity in rats through inhibition of TGF- β 1 and p-ERK1/2 axis. *Antioxidants (Basel, Switzerland)* **11**, 1499 (2022).
65. Parra Cid, T., Conejo García, J. R., Carballo Álvarez, F. & De Arriba, G. Antioxidant nutrients protect against cyclosporine A nephrotoxicity. *Toxicology* **189**, 99–111 (2003).
66. Redondo-Horcajo, M. *et al.* Cyclosporine A-induced nitration of tyrosine 34 MnSOD in endothelial cells: Role of mitochondrial superoxide. *Cardiovasc. Res.* **87**, 356–365 (2010).
67. Sattarinezhad, E. *et al.* Protective effect of edaravone against cyclosporine-induced chronic nephropathy through antioxidant and nitric oxide modulating pathways in rats. *Iran. J. Med. Sci.* **42**, 170–178 (2017).
68. Raeisi, S. *et al.* Oxidative stress-induced renal telomere shortening as a mechanism of cyclosporine-induced nephrotoxicity. *J. Biochem. Mol. Toxicol.* **32**, e22166 (2018).
69. Mohamadin, A. M., El-Beshbishy, H. A. & El-Mahdy, M. A. Green tea extract attenuates cyclosporine A-induced oxidative stress in rats. *Pharmacol. Res.* **51**, 51–57 (2005).
70. Tutanc, M. *et al.* Effects of erdosteine on cyclosporin-A-induced nephrotoxicity. *Hum. Exp. Toxicol.* **31**, 565–573 (2012).
71. Duru, M. *et al.* Protective effects of N-acetylcysteine on cyclosporine-A-induced nephrotoxicity. *Renal Fail.* **30**(4), 453–459. <https://doi.org/10.1080/08860220801985942> (2008).
72. Xiao, Z. *et al.* Mechanisms of cyclosporine-induced renal cell apoptosis: A systematic review. *Am. J. Nephrol.* **37**, 30–40 (2013).
73. Lai, Q. *et al.* Attenuation of cyclosporine A induced nephrotoxicity by schisandrin B through suppression of oxidative stress, apoptosis and autophagy. *Int. Immunopharmacol.* **52**, 15–23 (2017).
74. Donnahoo, K. K., Shames, B. D., Harken, A. H. & Meldrum, D. R. Review article: The role of tumor necrosis factor in renal ischemia-reperfusion injury. *J. Urol.* **162**, 196–203 (1999).
75. Adil, M., Kandhare, A. D., Visnagri, A. & Bodhankar, S. L. Naringin ameliorates sodium arsenite-induced renal and hepatic toxicity in rats: Decisive role of KIM-1, Caspase-3, TGF- β , and TNF- α . *Ren. Fail.* **37**, 1396–1407 (2015).
76. El-Bassossy, H., Hassanien, M., Bima, A., Ghoneim, F. & Elsamanoudy, A. Renal oxidative stress and inflammatory response in perinatal Cyclosporine-A exposed rat progeny and its relation to gender. *J. Microsc. Ultrastruct.* **7**, 44 (2019).
77. Hu, P., Han, Z., Couvillon, A. D., Kaufman, R. J. & Exton, J. H. Autocrine tumor necrosis factor alpha links endoplasmic reticulum stress to the membrane death receptor pathway through IRE1 α -mediated NF- κ B activation and down-regulation of TRAF2 expression. *Mol. Cell. Biol.* **26**, 3071–3084 (2006).
78. Han, S. W. *et al.* Prolonged endoplasmic reticulum stress induces apoptotic cell death in an experimental model of chronic cyclosporine nephropathy. *Am. J. Nephrol.* **28**, 707–714 (2008).
79. Al-Lamki, R. S. *et al.* TL1A both promotes and protects from renal inflammation and injury. *J. Am. Soc. Nephrol.* **19**, 953–960 (2008).
80. Arab, H. H. *et al.* Inhibition of oxidative stress and apoptosis by camel milk mitigates cyclosporine-induced nephrotoxicity: Targeting Nrf2/HO-1 and AKT/eNOS/NO pathways. *Food Sci. Nutr.* **9**, 3177–3190 (2021).
81. González-Guerrero, C. *et al.* TLR4-mediated inflammation is a key pathogenic event leading to kidney damage and fibrosis in cyclosporine nephrotoxicity. *Arch. Toxicol.* **91**, 1925–1939 (2017).
82. Yang, C. W. *et al.* Expression of apoptosis-related genes in chronic cyclosporine nephrotoxicity in mice. *Am. J. Transplant.* **2**, 391–399 (2002).
83. Liu, Z. *et al.* Sesamol induces human hepatocellular carcinoma cells apoptosis by impairing mitochondrial function and suppressing autophagy. *Sci. Rep.* **7**, 45728 (2017).
84. Ahmadvand, H., Nouryazdan, N., Nasri, M., Adibhesami, G. & Babaenezhad, E. Renoprotective effects of gallic acid against gentamicin nephrotoxicity through amelioration of oxidative stress in rats. *Braz. Arch. Biol. Technol.* **63**, 1–13 (2020).
85. Babaenezhad, E. *et al.* Exogenous glutathione protects against gentamicin-induced acute kidney injury by inhibiting NF- κ B pathway, oxidative stress, and apoptosis and regulating PCNA. *Drug Chem. Toxicol.* **46**, 441–450 (2023).
86. Shihab, F. S., Andoh, T. F., Tanner, A. M., Yi, H. & Bennett, W. M. Expression of apoptosis regulatory genes in chronic cyclosporine nephrotoxicity favors apoptosis. *Kidney Int.* **56**, 2147–2159 (1999).
87. Huang, J., Yao, X., Weng, G., Qi, H. & Ye, X. Protective effect of curcumin against cyclosporine A-induced rat nephrotoxicity. *Mol. Med. Rep.* **17**, 6038–6044 (2018).
88. Temel, Y., Kucukler, S., Yildirim, S., Caglayan, C. & Kandemir, F. M. Protective effect of chrysin on cyclophosphamide-induced hepatotoxicity and nephrotoxicity via the inhibition of oxidative stress, inflammation, and apoptosis. *Naunyn. Schmiedeberg's Arch. Pharmacol.* **393**, 325–337 (2020).
89. Chiu, P. Y., Chen, N., Leong, P. K., Leung, H. Y. & Ko, K. M. Schisandrin B elicits a glutathione antioxidant response and protects against apoptosis via the redox-sensitive ERK/Nrf2 pathway in H9c2 cells. *Mol. Cell. Biochem.* **350**, 237–250 (2011).
90. Xiong, L. *et al.* The Activation of Nrf2 and its downstream regulated genes mediates the antioxidative activities of Xueshuan Xinmaining tablet in human umbilical vein endothelial Cells. *Evid. Based. Complement. Alternat. Med.* **2015**, (2015).
91. Ortega-Trejo, J. A. *et al.* Effect of fosfomicin on cyclosporine nephrotoxicity. *Antibiot. (Basel, Switzerland)* **9**, 1–14 (2020).
92. Jin, M. *et al.* Klotho ameliorates cyclosporine A-induced nephropathy via PDLIM2/NF- κ B p65 signaling pathway. *Biochem. Biophys. Res. Commun.* **486**, 451–457 (2017).
93. Hammoud, S. H. *et al.* Molecular basis of the counteraction by calcium channel blockers of cyclosporine nephrotoxicity. *Am. J. Physiol. Renal Physiol.* **315**, F572–F582 (2018).
94. Arab, H. H., Ashour, A. M., Alqarni, A. M., Arafa, E. S. A. & Kabel, A. M. Camel milk mitigates cyclosporine-induced renal damage in rats: Targeting p38/ERK/JNK MAPKs, NF- κ B, and matrix metalloproteinases. *Biology (Basel)* **10**, 442 (2021).
95. Gur, C., Kandemir, F. M., Caglayan, C. & Satıcı, E. Chemopreventive effects of hesperidin against paclitaxel-induced hepatotoxicity and nephrotoxicity via amendment of Nrf2/HO-1 and caspase-3/Bax/Bcl-2 signaling pathways. *Chem. Biol. Interact.* **365**, 110073 (2022).
96. Rajan, P. *et al.* Anti-diabetic effect of hesperidin on palmitate (PA)-treated HepG2 cells and high fat diet-induced obese mice. *Food Res. Int.* **162**, 112059 (2022).
97. El-Shahawy, A. A. G., Abdel-Moneim, A., Ebeid, A. S. M., Eldin, Z. E. & Zanaty, M. I. A novel layered double hydroxide-hesperidin nanoparticles exert antidiabetic, antioxidant and anti-inflammatory effects in rats with diabetes. *Mol. Biol. Rep.* **48**, 5217–5232 (2021).
98. Sundaram, R., Nandhakumar, E. & Haseena Banu, H. Hesperidin, a citrus flavonoid ameliorates hyperglycemia by regulating key enzymes of carbohydrate metabolism in streptozotocin-induced diabetic rats. *Toxicol. Mech. Methods* **29**(9), 644–653. <https://doi.org/10.1080/15376516.2019.164637> (2019).
99. Kamel, K. M., Abd El-Raouf, O. M., Metwally, S. A., Abd El-Latif, H. A. & El-sayed, M. E. Hesperidin and rutin, antioxidant citrus flavonoids, attenuate cisplatin-induced nephrotoxicity in rats. *J. Biochem. Mol. Toxicol.* **28**, 312–319 (2014).
100. Nathiya, S., Rajaram, S. & Abraham, P. Hesperidin alleviates antitubercular drug induced oxidative stress, inflammation and apoptosis in rat liver. *Int. J. Biomed. Res.* <https://doi.org/10.7439/IJBR.V7I7.3414> (2016).
101. Ahmad, S. T. *et al.* Hesperidin alleviates acetaminophen induced toxicity in Wistar rats by abrogation of oxidative stress, apoptosis and inflammation. *Toxicol. Lett.* **208**, 149–161 (2012).
102. Siddiqi, A., Nafees, S., Rashid, S., Sultana, S. & Saidullah, B. Hesperidin ameliorates trichloroethylene-induced nephrotoxicity by abrogation of oxidative stress and apoptosis in wistar rats. *Mol. Cell. Biochem.* **406**, 9–20 (2015).

103. Morsy, M. A., El-Sheikh, A. A. K., Ibrahim, A. R. N. & El-Daly, M. Protection of hesperidin against methotrexate-induced nephrotoxicity may be mediated by Nrf2/HO-1 pathway. *Indian J. Pharm. Educ. Res.* **55**, 1066–1073 (2021).
104. Elavarasan, J. *et al.* Hesperidin-mediated expression of Nrf2 and upregulation of antioxidant status in senescent rat heart. *J. Pharm. Pharmacol.* **64**, 1472–1482 (2012).
105. Mahmoud, A. M., Mohammed, H. M., Khadrawy, S. M. & Galaly, S. R. Hesperidin protects against chemically induced hepatocarcinogenesis via modulation of Nrf2/ARE/HO-1, PPAR γ and TGF- β 1/Smad3 signaling, and amelioration of oxidative stress and inflammation. *Chem. Biol. Interact.* **277**, 146–158 (2017).
106. Subramanian, P., Anandan, R., Jayapalan, J. J. & Hashim, O. H. Hesperidin protects gentamicin-induced nephrotoxicity via Nrf2/HO-1 signaling and inhibits inflammation mediated by NF- κ B in rats. *J. Funct. Foods* **13**, 89–99 (2015).
107. Aly, M. S. *et al.* Hesperidin protects against diethylnitrosamine/carbon tetrachloride-induced renal repercussions via up-regulation of Nrf2/HO-1 signaling and attenuation of oxidative stress. *J. Appl. Pharm. Sci.* **7**, 007–014 (2017).
108. Aroor, A. R., Manrique-Acevedo, C. & DeMarco, V. G. The role of dipeptidylpeptidase-4 inhibitors in management of cardiovascular disease in diabetes; focus on linagliptin. *Cardiovasc. Diabetol.* **17**, 1–15 (2018).
109. Lovshin, J. A. & Zinman, B. Blood pressure-lowering effects of incretin-based diabetes therapies. *Can. J. Diabetes* **38**, 364–371 (2014).
110. Mulvihill, E. E. & Drucker, D. J. Pharmacology, physiology, and mechanisms of action of dipeptidyl peptidase-4 inhibitors. *Endocr. Rev.* **35**, 992–1019 (2014).
111. Von Websky, K., Reichetzeder, C. & Hochoer, B. Physiology and pathophysiology of incretins in the kidney. *Curr. Opin. Nephrol. Hypertens.* **23**, 54–60 (2014).
112. Li, J. *et al.* The dipeptidyl peptidase-4 inhibitor sitagliptin protects against dyslipidemia-related kidney injury in Apolipoprotein E knockout mice. *Int. J. Mol. Sci.* **15**, 11416–11434 (2014).
113. Vaghasiya, J., Sheth, N., Bhalodia, Y. & Manek, R. Sitagliptin protects renal ischemia reperfusion induced renal damage in diabetes. *Regul. Pept.* **166**, 48–54 (2011).
114. Marques, C. *et al.* Sitagliptin prevents inflammation and apoptotic cell death in the kidney of type 2 diabetic animals. *Mediators Inflamm.* **2014**, (2014).
115. Abuelezz, S. A., Hendawy, N. & Abdel Gawad, S. Alleviation of renal mitochondrial dysfunction and apoptosis underlies the protective effect of sitagliptin in gentamicin-induced nephrotoxicity. *J. Pharm. Pharmacol.* **68**, 523–532 (2016).
116. Shalaby, A. Renoprotective effect of sitagliptin (dipeptidyl peptidase-4 inhibitor) against cisplatin induced nephrotoxicity in mice. *Br. J. Pharm. Res.* **4**, 1116–1129 (2014).
117. Deger, M. *et al.* Protective effect of dapagliflozin against cyclosporine A-induced nephrotoxicity. *Drug Chem. Toxicol.* **45**, 2637–2643 (2022).
118. Nuransoy, A. *et al.* Protective effect of sitagliptin against renal ischemia reperfusion injury in rats. *Ren. Fail.* **37**, 687–693 (2015).
119. Apaijai, N., Pintana, H., Chattipakorn, S. C. & Chattipakorn, N. Effects of vildagliptin versus sitagliptin, on cardiac function, heart rate variability and mitochondrial function in obese insulin-resistant rats. *Br. J. Pharmacol.* **169**, 1048–1057 (2013).
120. Pintana, H., Apaijai, N., Chattipakorn, N. & Chattipakorn, S. C. DPP-4 inhibitors improve cognition and brain mitochondrial function of insulin-resistant rats. *J. Endocrinol.* **218**, 1–11 (2013).
121. Alam, M. A., Hasan Chowdhury, M. R., Jain, P., Sagor, M. A. T. & Reza, H. M. DPP-4 inhibitor sitagliptin prevents inflammation and oxidative stress of heart and kidney in two kidney and one clip (2K1C) rats. *Diabetol. Metab. Syndr.* **7**, 107 (2015).
122. Nader, M. A., El-Awady, M. S., Shalaby, A. A. & El-Agamy, D. S. Sitagliptin exerts anti-inflammatory and anti-allergic effects in ovalbumin-induced murine model of allergic airway disease. *Naunyn. Schmiedebergs. Arch. Pharmacol.* **385**, 909–919 (2012).
123. Fan, L. *et al.* Sitagliptin protects against hypoxia / reoxygenation (H / R) -induced cardiac microvascular endothelial cell injury. *Am. J. Transl. Res.* **11**, 2099–2107 (2019).
124. Esposito, G. *et al.* Sitagliptin reduces inflammation, fibrosis and preserves diastolic function in a rat model of heart failure with preserved ejection fraction. *Br. J. Pharmacol.* **174**, 4070 (2017).
125. Tsaia, T. H. *et al.* Sitagliptin attenuated brain damage and cognitive impairment in mice with chronic cerebral hypo-perfusion through suppressing oxidative stress and inflammatory reaction. *J. Hypertens.* **33**, 1001–1013 (2015).
126. El-Sahar, A. E., Safar, M. M., Zaki, H. F., Attia, A. S. & Ain-Shoka, A. A. Sitagliptin attenuates transient cerebral ischemia/reperfusion injury in diabetic rats: Implication of the oxidative-inflammatory-apoptotic pathway. *Life Sci.* **126**, 81–86 (2015).
127. Kong, L. *et al.* Sitagliptin activates the p62-Keap1-Nrf2 signalling pathway to alleviate oxidative stress and excessive autophagy in severe acute pancreatitis-related acute lung injury. *Cell Death Dis.* **12**, 928 (2021).
128. Zhang, Q. *et al.* Sitagliptin ameliorates renal tubular injury in diabetic kidney disease via STAT3-dependent mitochondrial homeostasis through SDF-1 α /CXCR4 pathway. *FASEB J.* **34**, 7500–7519 (2020).
129. Taha, M. *et al.* Palliative role of Zamzam water against cyclosporine-induced nephrotoxicity through modulating autophagy and apoptosis crosstalk. *Toxics* **11**, 377 (2023).
130. El-Agamy, D. S., Abo-Haded, H. M. & Elkablawy, M. A. Cardioprotective effects of sitagliptin against doxorubicin-induced cardiotoxicity in rats. *Exp. Biol. Med. (Maywood)* **241**, 1577–1587 (2016).
131. Abdelrahman, R. S. Sitagliptin exerts anti-apoptotic effect in nephrotoxicity induced by cisplatin in rats. *Naunyn. Schmiedebergs. Arch. Pharmacol.* **390**, 721–731 (2017).
132. Ohkawa, H., Ohishi, N. & Yagi, K. Assay for lipid peroxides in animal tissues by thiobarbituric acid reaction. *Anal. Biochem.* **95**, 351–358 (1979).
133. Beutler, E., Duron, O. & Kelly, B. M. Improved method for the determination of blood glutathione. *J. Lab. Clin. Med.* **61**, 882–888 (1963).
134. Aebi, H. Catalase in vitro. *Methods Enzymol.* **105**, 121–126 (1984).
135. Sun, Y. I., Oberley, L. W. & Li, Y. A simple method for clinical assay of superoxide dismutase. *Clin. Chem.* **34**(3), 497–500 (1988).
136. Toghan, R. *et al.* Protective effects of Folic acid against reproductive, hematological, hepatic, and renal toxicity induced by Acetamidiprid in male Albino rats. *Toxicology* **469**, 153115 (2022).
137. Saleh, S. M. M., Mahmoud, A. B., Al-Salahy, M. B. & Mohamed Moustafa, F. A. Morphological, immunohistochemical, and biochemical study on the ameliorative effect of gallic acid against bisphenol A-induced nephrotoxicity in male albino rats. *Sci. Rep.* **13**, 1732 (2023).
138. Dries, D. J. Histological and histochemical methods. *Shock* **30**, 481 (2008).
139. Abd-Eldayem, A. M., Alnasser, S. M., Abd-Elhafeez, H. H., Soliman, S. A. & Abdel-Emam, R. A. Therapeutic versus preventative use of ginkgo biloba extract (EGb 761) against indomethacin-induced gastric ulcer in mice. *Molecules* **27**, 5598 (2022).

Author contributions

Material preparation, data collection, and analysis were performed by Basim Anwar Shehata Messiha, [Ahmed M. Abd-Eldayem, Sohayla Mahmoud Makram, Hanan H. Abd-Elhafeez, Mustafa Ahmed Abdel-Reheim. The first draft of the manuscript was written by Ahmed M. Abd-Eldayem, Sohayla Mahmoud Makram, and Hanan H. Abd-Elhafeez. Final review and editing by Basim Anwar Shehata Messiha, [Ahmed M. Abd-Eldayem, Sohayla Mahmoud Makram. All authors reviewed the manuscript.

Funding

Open access funding provided by The Science, Technology & Innovation Funding Authority (STDF) in cooperation with The Egyptian Knowledge Bank (EKB). The authors declare that no funds, grants, or other support were received.

Competing interests

The authors declare no competing interests.

Additional information

Supplementary Information The online version contains supplementary material available at <https://doi.org/10.1038/s41598-024-57300-x>.

Correspondence and requests for materials should be addressed to A.M.A.-E.

Reprints and permissions information is available at www.nature.com/reprints.

Publisher's note Springer Nature remains neutral with regard to jurisdictional claims in published maps and institutional affiliations.



Open Access This article is licensed under a Creative Commons Attribution 4.0 International License, which permits use, sharing, adaptation, distribution and reproduction in any medium or format, as long as you give appropriate credit to the original author(s) and the source, provide a link to the Creative Commons licence, and indicate if changes were made. The images or other third party material in this article are included in the article's Creative Commons licence, unless indicated otherwise in a credit line to the material. If material is not included in the article's Creative Commons licence and your intended use is not permitted by statutory regulation or exceeds the permitted use, you will need to obtain permission directly from the copyright holder. To view a copy of this licence, visit <http://creativecommons.org/licenses/by/4.0/>.

© The Author(s) 2024